Journal of South American Earth Sciences 42 (2013) 260–276

Contents lists available at SciVerse ScienceDirect

Journal of South American Earth Sciences

journal homepage: www.elsevier.com/locate/jsames

Seismic structure of the crust and uppermost mantle of South America and surrounding oceanic basins

Gary S. Chulick [a], Shane Detweiler [b,*], Walter D. Mooney [b]

[a] Mt. Aloysius College, 7373 Admiral Peary Hwy, Cresson, PA 16630, USA
[b] United States Geological Survey, MS 977, 345 Middlefield Road, Menlo Park, CA 94025, USA

ARTICLE INFO

Article history:
Received 19 July 2011
Accepted 5 June 2012

Keywords:
Crustal structure
Seismic velocity
South America

ABSTRACT

We present a new set of contour maps of the seismic structure of South America and the surrounding ocean basins. These maps include new data, helping to constrain crustal thickness, whole-crustal average P-wave and S-wave velocity, and the seismic velocity of the uppermost mantle (P_n and S_n). We find that: (1) The weighted average thickness of the crust under South America is 38.17 km (standard deviation, s.d. ±8.7 km), which is ~1 km thinner than the global average of 39.2 km (s.d. ±8.5 km) for continental crust. (2) Histograms of whole-crustal P-wave velocities for the South American crust are bi-modal, with the lower peak occurring for crust that appears to be missing a high-velocity (6.9–7.3 km/s) lower crustal layer. (3) The average P-wave velocity of the crystalline crust (P_{cc}) is 6.47 km/s (s.d. ±0.25 km/s). This is essentially identical to the global average of 6.45 km/s. (4) The average P_n velocity beneath South America is 8.00 km/s (s.d. ±0.23 km/s), slightly lower than the global average of 8.07 km/s. (5) A region across northern Chile and northeast Argentina has anomalously low P- and S-wave velocities in the crust. Geographically, this corresponds to the shallowly-subducted portion of the Nazca plate (the Pampean flat slab first described by Isacks et al., 1968), which is also a region of crustal extension. (6) The thick crust of the Brazilian craton appears to extend into Venezuela and Colombia. (7) The crust in the Amazon basin and along the western edge of the Brazilian craton may be thinned by extension. (8) The average crustal P-wave velocity under the eastern Pacific seafloor is higher than under the western Atlantic seafloor, most likely due to the thicker sediment layer on the older Atlantic seafloor.

Published by Elsevier Ltd.

1. Introduction

The construction of continent-scale maps of geophysical properties provides a broad picture of the structure of the Earth. For example, a map of crustal thickness indicates the lateral extent of tectonic provinces such as highly extended regions and orogenic zones. Likewise, maps of crustal seismic velocities can help to delineate platforms, shields, sedimentary basins, and exotic accreted terrains (Christensen and Mooney, 1995). Geophysical maps provide a means of identifying crustal properties that delineate geologic provinces (e.g., Prodehl, 1984; Meissner, 1986; Collins, 1988; Pakiser and Mooney, 1989; Blundell et al., 1992; Pavlenkova, 1996; Yuan, 1996; Chulick and Mooney, 2002; Fuck et al., 2008; Cordani et al., 2009; Cordani et al., 2010).

We present the first set of contour maps based on seismic-refraction work combined with other forms of seismic data (i.e., seismic reflection, sonobuoy, receiver function and earthquake models) for the entire continent of South America and the surrounding ocean basins. There are several reasons why new maps are warranted at this time. First, the quantity and quality of data on South American crustal structure has grown substantially in the past decade or so, with new seismic surveys (e.g. Wigger et al., 1994; Flueh et al., 1998; Patzwahl et al., 1999; Bohm et al., 2002; ANCORP Working Group, 2003; Berrocal et al., 2004; Schmitz et al., 2005; Rodger et al., 2006; Scherwath et al., 2006; Soares et al., 2006; Greenroyd et al., 2007) conducted that cover hitherto unexplored regions (e.g. the Chilean Andes and Amazonia) as well as provide better resolution in previously studied areas (e.g., the Peruvian Andes, and eastern Brazil). However, this work in South America has generally not been done at the continental scale and frequently depends on passive source data (e.g. Schmitz et al., 1999; Assumpção et al., 2002, 2004; An and Assumpção, 2005; Tavera et al., 2006; Lange et al., 2007; Heit et al., 2008; Wölbern et al., 2009). This study consolidates the

* Corresponding author. Tel.: +1 650 329 5192; fax: +1 650 329 5163.
E-mail address: shane@usgs.gov (S. Detweiler).

0895-9811/$ – see front matter Published by Elsevier Ltd.
http://dx.doi.org/10.1016/j.jsames.2012.06.002

work of previous studies by combining different types of crustal structure data taken from throughout the continent, including numerous geological provinces and tectonic regimes. The main geologic provinces of South America are shown in Fig. 1.

We also present contour maps and statistical analyses of the S-wave velocity of the crust and Moho of South America. Such presentations are particularly relevant given the recent publication of tomographic S-wave velocity maps of the South American mantle (e.g. van der Lee et al., 2001, 2002; Feng et al., 2004, 2007).

Our newly-collected data, mentioned above, have been incorporated into a comprehensive seismic database (website address provided at the end of the article). Each data point used in this study consists of a one-dimensional velocity-depth function extracted from a published crustal model. More than 75% of the data points were taken from 2D seismic velocity cross sections derived from seismic-refraction data. Every effort has been made to include results published through 2011; however, some important and/or recently-completed seismic surveys are not fully available. Nonetheless, we can for the first time produce reasonably detailed maps of P-wave crustal properties for all of South America, as well as corresponding generalized maps of S-wave crustal properties. The locations for all seismic data points used in this study are shown in Fig. 2.

The maps presented here include crustal thickness (H_c), average P-wave velocity of the whole crust (P_c) and of the crystalline crust (P_{cc}), sub-Moho P-wave velocity (P_n), average S-wave velocity of the whole crust (S_c) and of the crystalline crust (S_{cc}), and sub-Moho S-wave velocity (S_n). Furthermore we provide a statistical analysis of these parameters, as well as of the velocity ratios P_c/S_c, P_{cc}/S_{cc}, and P_n/S_n. We also present several crustal cross-sections through the South American continent synthesized from our velocity data compilation.

2. Previous work

Maps of deep crustal properties for South America based on seismic-refraction data have hitherto been limited in extent, primarily to local regions of the Andes (e.g. Wigger et al., 1994; Schmitz, 1994; Bohm et al., 2002; ANCORP Working Group, 2003; Alvarado et al., 2005; Gilbert et al., 2006; Alvarado et al., 2007; Yoon et al., 2009)

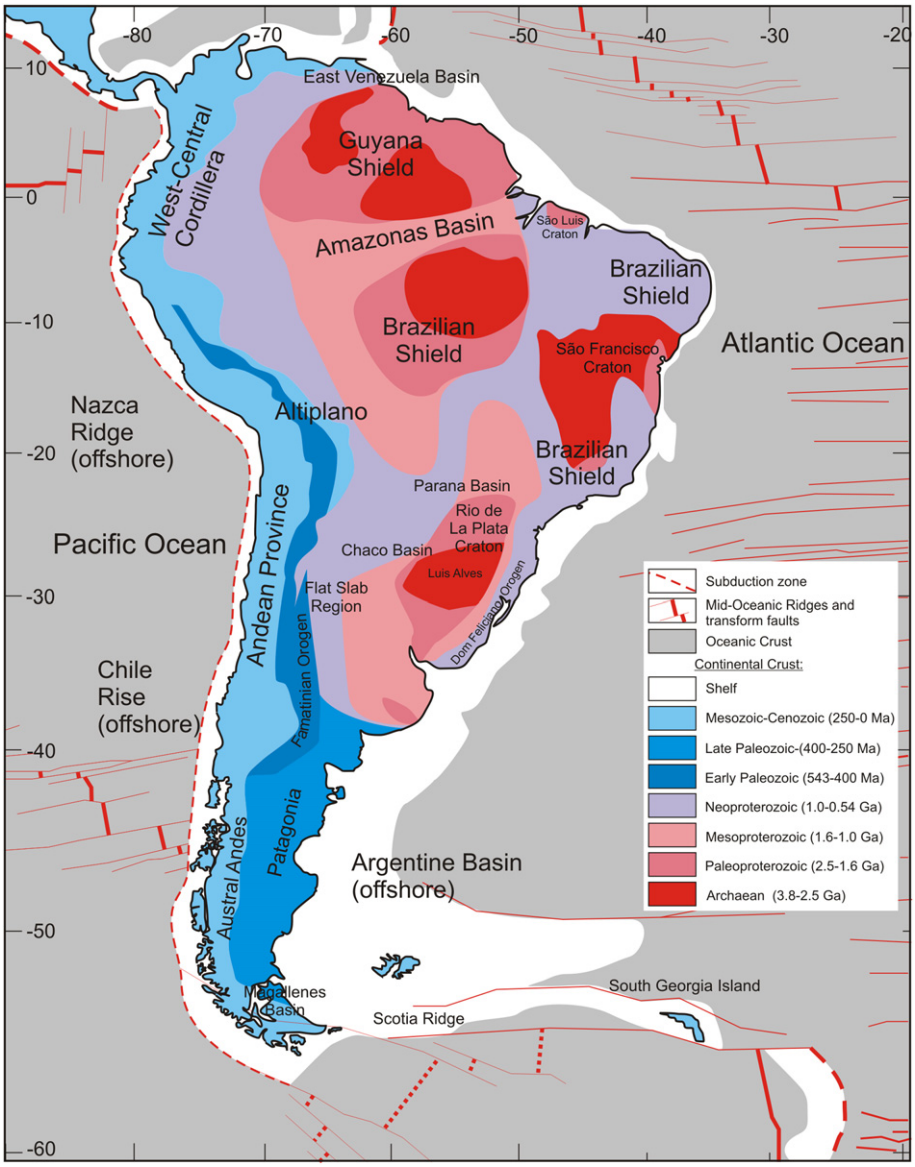

Fig. 1. Main Geological Provinces of South America. (After Gubanov and Mooney, pers. comm., 2012).

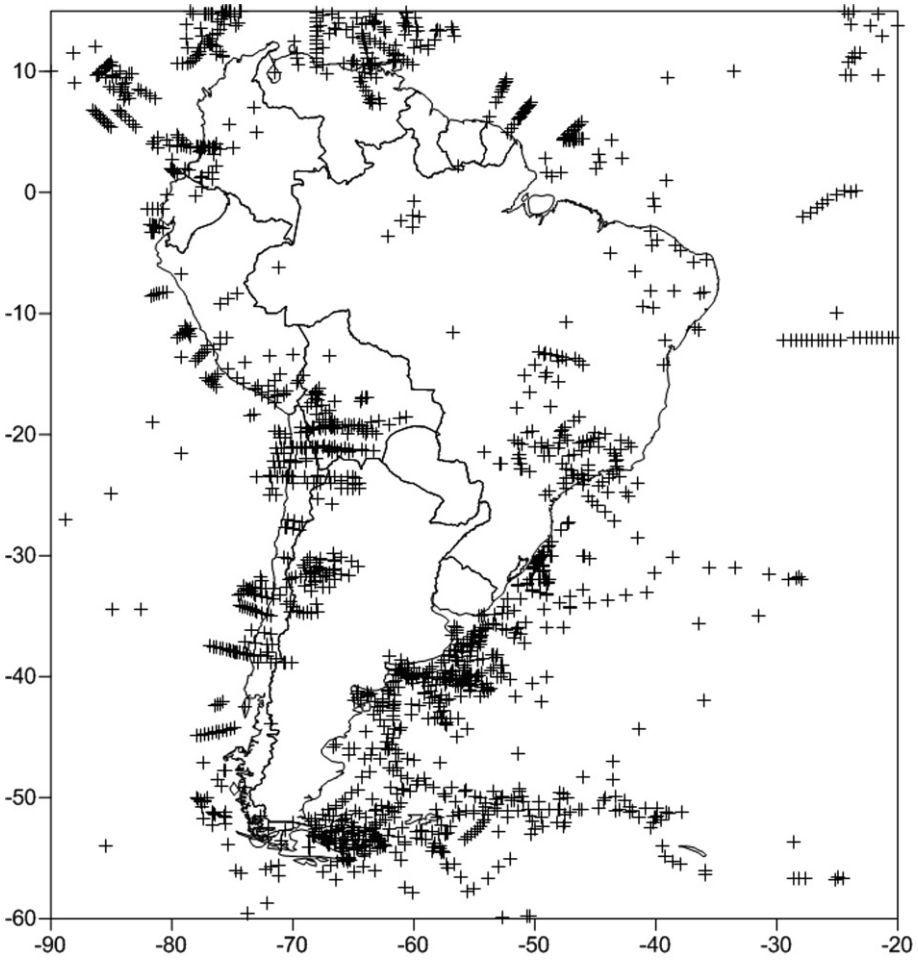

Fig. 2. Location map for the one-dimensional seismic data profiles used in this study. See: http://earthquake.usgs.gov/research/structure/crust/sam.php for details.

and the continental margins (e.g. Bezada et al., 2008; Christeson et al., 2008; Agudelo et al., 2009; Pavlenkova et al., 2009). Some local modeling studies using surface waves have also been performed, principally in Brazil (e.g. Nascimento et al., 2002; Assumpção et al., 2002, 2004; An and Assumpção, 2004; Blaich et al., 2008; Julia et al., 2008) and Argentina (e.g. Schnabel, 2007; Blaich et al., 2009).

The first true continent-scale maps of crustal thickness, and sub-Moho S-wave velocities for South America were produced by van der Lee et al. (2001, 2002) and Feng et al. (2004, 2007), using body-wave tomography that had been constrained by surface waves. Crust 2.0 (Bassin et al., 2000) was done at global scale, but still contained decent coverage of South America. Here we go one step further by producing the first continental-scale maps of crustal P-wave and S-wave velocities for South America based on a combination of seismic refraction and reflection surveys, surface wave analyses, tomography and other forms of seismic data, in a manner analogous to our study of North America (Chulick and Mooney, 2002). Thus, for example, our model for the South American crustal thickness may be compared to the results of Crust 2.0 (Bassin et al., 2000), van der Lee et al. (2001, 2002), and Lloyd et al. (2010).

3. Data and uncertainties

We have compiled a catalog of the seismic structure of the crust and uppermost mantle of South America and the surrounding oceans that includes all types of seismic data, including refraction and reflection profiling, surface-wave and receiver function analysis, and local earthquake tomography (Chulick, 1997). Our South American catalog currently contains 889 velocity-depth functions ("data points"), though ~25% of these do not reach Moho depths. Of those that do model the entire crust, we have used 658 in the present study. About 75% of these utilized velocity-depth functions were derived from seismic-refraction data. Given the ambiguity in identifying the thickness of sediments for each individual data point, we have adopted a velocity horizon to define the depth of the top of the crystalline or "consolidated" crust. A P-wave value of 5.8 km/s was chosen for this seismic velocity horizon for P-wave functions as it is higher than the velocity in most sedimentary rocks, but lower than the minimum velocity (~5.9 km/s) found in virtually all granitic rocks. Similarly, an S-wave value of 3.35 km/s was chosen as the corresponding velocity horizon for S-wave functions.

The accuracy of the generated contour maps is strongly affected by the uncertainties in the published interpretations of crustal structure. Useful reviews of the uncertainties associated with the methods utilized to determine the structure of the crust and sub-crustal lithosphere are provided by Mooney (1989) and Bostock (1999). The uncertainties in crustal models arise from such factors as the survey method, the spatial resolution of the survey (e.g., the spacing of the shot points and the recording stations), and the analytical techniques used to process the data. Typically, the uncertainty in the calculated depth of the Moho is approximately 5–10%. Thus, a reported crustal thickness of 40 km has an

uncertainty of ±2–4 km. The seismic velocities determined from refracted first-arrivals (e.g., P_n) are typically accurate to within a few hundredths of a km/s (Mooney, 1989; Chulick, 1997).

4. Results

South American geological provinces and place names are presented in Fig. 1, while the locations of the compiled P- and S-wave velocity-depth functions are shown in Fig. 2. Statistical analyses for each of the seismic parameters are presented in Tables 1 and 2. The data types (seismic refraction, receiver function, etc.) and data quantity used in the construction of the maps are presented in Table 3. The contour maps presented in Figs. 3–9 were constructed using commercial software employing the natural-neighbor technique for gridding. Certain regions with very sparse data (e.g., the Amazonas Basin) yielded unreasonable contours. Where possible, we edited these regional results to avoid obvious geographical errors, such as oceanic crustal thickness appearing on continental crust. The data used are available at the Web address provided at the end of this article.

4.1. Crustal thickness (H_c)

Our map (Fig. 3) demonstrates not only the extraordinary thickness but also the variation found in the continental crust beneath the Andes. The crust under the central Andes appears to form a single block that is extremely thick, exceeding 60 km from central Peru south through western Bolivia into northern Chile. Since this region corresponds geographically to the Altiplano, we interpret the Altiplano to be a continental plateau underlain by extremely thick continental crust along a convergent margin. This suggests that it is a structural analog to the southern Tibetan Plateau.

In central Chile the crust under the Andes is also very thick (>50 km; see Wagner et al., 2005; Heit et al., 2008; Yoon et al., 2009; Lloyd et al., 2010). However, farther south, in the Austral Andes of southern Chile and Patagonia, the crust thins gradually; in the region of Tierra del Fuego, the crust is only about 30 km thick (Lawrence and Wiens, 2004; Lloyd et al., 2010).

To the north of central Peru, there is far less crustal seismic data than for areas further to the south (James and Snoke, 1994). However, the seismic refraction surveys and earthquake modeling that has been done also shows variations in crustal thickness under the northern Andes (Ocola et al., 1975). In northern Peru, there is evidence that the crust thins to nearly 40 km, but further to the north it thickens again to at least 50 km under Colombia and western Venezuela (Mooney et al., 1979; Schmitz et al., 2005).

Fig. 3 further indicates a moderately thick (>40 km) crust under the Guiana and Brazilian Shields (Fig. 1), with clear indications that the crust is thinner (~35 km) to the west, under the central part of the continent. This moderately thick (~35 km) crust is consistent with previous studies (e.g. Soares et al., 2006) and has been seen under other shields as well (e.g. the Canadian Shield (35–50 km), Eaton et al., 2005; the Baltic Shield (35–55 km), Balling, 1995). The

Table 1
Comparison of statistical analyses of Chulick and Mooney (2002) (North America), Christensen and Mooney (1995) (global), and this study (South America). H_c = crustal thickness; P_{cc} (S_{cc}) = average P-wave (S-wave) velocity of the crystalline crust (i.e., below sediments); P_n (S_n) = P-wave (S-wave) velocity of the uppermost mantle. n = number of data points; x = average value, $\pm\sigma$ = standard deviation. The statistical error, $\pm e = [\sigma \div$ square root of $n]$.

	Chulick and Mooney (North Am.) [2002]	Christensen and Mooney (Global) [1995]	This study (S. Am. continental crust only)	This study (all crust)
H_c (km)				
n	337	560	526	
x	36.10	39.17	43.83	
$\pm\sigma$	8.97	8.52	13.97	
$\pm e$	0.48	0.36	0.609	
P_{cc} (km/s)				
n	255	560	346	643
X	6.435	6.45	6.467	6.580
$\pm\sigma$	0.235	0.23	0.245	0.280
$\pm e$	0.015	0.01	0.013	0.011
S_{cc} (km/s)				
n	67		140	151
X	3.639		3.698	3.706
$\pm\sigma$	0.163		0.150	0.159
$\pm e$	0.02		0.013	0.013
P_n (km/s)				
n	320	560	355	658
X	8.018	8.07	7.998	8.013
$\pm\sigma$	0.205	0.21	0.227	0.227
$\pm e$	0.01	0.01	0.012	0.009
S_n (km/s)				
n	76		79	90
x	4.471		4.504	4.495
$\pm\sigma$	0.165		0.154	0.160
$\pm e$	0.019		0.017	0.017

Table 2
Statistical analyses of the crustal and mantle parameters presented in this study. H_c = crustal thickness; P_c (S_c) = average P-wave (S-wave) velocity of the whole crust (i.e., including sediments); P_{cc} (S_{cc}) = average P-wave (S-wave) velocity of the crystalline crust (i.e., below sediments); P_n (S_n) = P-wave (S-wave) velocity of the uppermost mantle.

Parameter	Average	Standard deviation	Number of data points
H_c [continental] (km)	43.83	13.97	526
H_c [oceanic] (km)	11.86	6.678	363
P_c [continental] (km/s)	6.191	0.377	347
P_c [oceanic] (km/s)	5.565	0.707	303
P_{cc} [continental] (km/s)	6.467	0.245	346
P_{cc} [oceanic] (km/s)	6.712	0.259	297
P_n [continental] (km/s)	7.998	0.227	355
P_n [oceanic] (>7.5 km/s)	8.032	0.225	303
S_c [continental] (km/s)	3.587	0.156	142
S_{cc} [continental] (km/s)	3.698	0.150	140
S_n [continental] (km/s)	4.504	0.154	79
P_c/S_c [continental]	1.748	0.0776	77
P_{cc}/S_{cc} [continental]	1.745	0.0575	75
P_n/S_n [continental]	1.771	0.0433	79

Table 3
Distribution of data points for each crustal and uppermost mantle parameter mapped in this study according to crustal type and source method. H_c = crustal thickness; P_c (S_c) = average P-wave (S-wave) velocity of the whole crust (i.e., including sediments); P_n (S_n) = P-wave (S-wave) velocity of the uppermost mantle.

	H_c	P_c	P_n	S_c	S_n
Total number of control points	889	643	658	154	90
Number of continental control points	526	346	355	142	79
Number of oceanic control points	363	297	303	12	11
Control points from					
Reversed seismic refraction surveys	403	349	355	8	10
Unreversed seismic refraction surveys	91	79	79	7	5
Sonobuoys	14	14	14	0	0
Split seismic refraction surveys	17	17	17	0	0
Receiver functions or earthquake models	272	132	132	94	54
Time-term analysis of seismic refr. data	0	0	0	0	0
Tomographic inversion	43	42	42	11	11
Surface wave analysis	36	8	10	34	10
Other methods	13	2	9	0	0

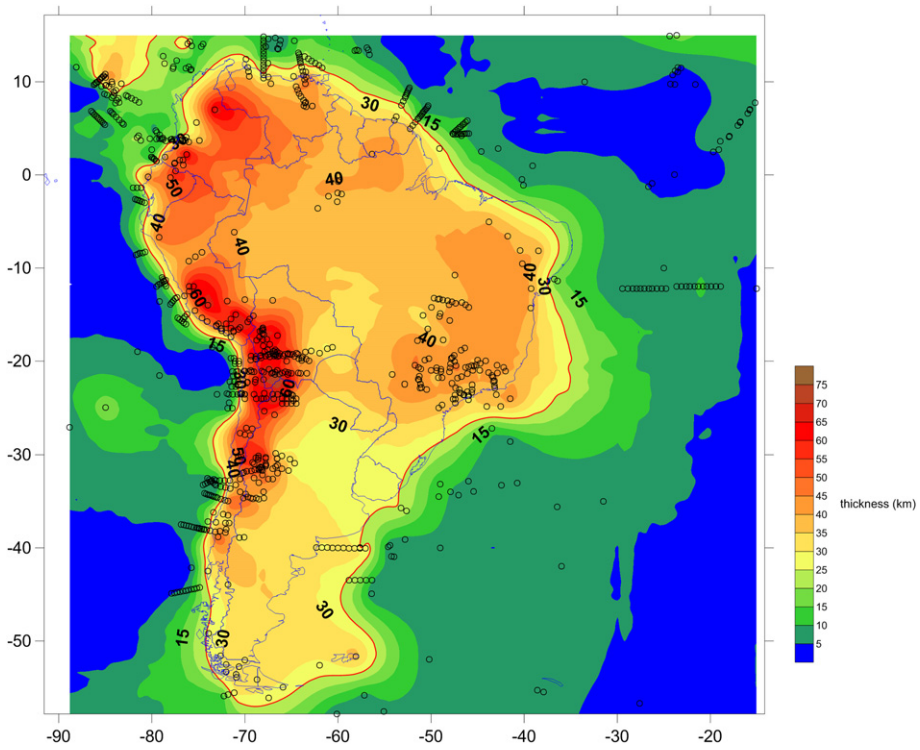

Fig. 3. Contour map of crustal thickness (H_c) of South America and adjacent ocean basins derived from seismic data. Among the many details, the map indicates the thinner crust west of the thick craton, and the map documents the well-known extraordinary thickness along much of the length of the Andes (>50 km), with clear indication that this thickness gradually decreases southwards (from ~50 km under central Chile to ~30 km beneath Tierra del Fuego). The red line highlights the 25 km contour which delineates the landward edge of the continental margins of South America. The western margin (the zone between the 10 km and 30 km contour lines) is narrow (<100 km), whereas the eastern margin is much wider (up to 1000 km or more). See Fig. 1 for location of place names.

exact degree of westward thinning will not be certain until extensive deep seismic work is done in the Amazonas and Chaco Basins, and along the lower valley and estuary of the Rio de la Plata (Fig. 1).

The increased data along the north coast of South America (primarily from BOLIVAR & Guianan Surveys) and Chile (various) do give better definition to the correlation between the continental margin and continental crust. Contrarily, the data in southeastern Brazil clearly indicate that the Moho is poorly contoured along the coast of central Brazil – this region has only seismic reflection surveys and a few analyses of surface waves, but no seismic refraction, earthquake tomography, nor receiver function models.

This pattern of crustal thickness is more consistent with the tomographic S-wave model 3SMAC (Nataf and Richard, 1996) than CRUST 2.0 (Bassin et al., 2000); the latter was based on an older, much less extensive version of our database than used in the current study. Our results are also consistent with the SA99 Moho map from S-wave tomography of van der Lee et al. (2001, 2002). Several features that we noted above on our map also appear on their map, including the Altiplano as a single very thick unit, the thinner crust in northern Peru, and the north-south elongated, thinned crust between the Andes and the cratons.

A comparison to the Moho map of Lloyd et al. (2010) also shows our results to be in general agreement where thickness can be constrained by data. Lloyd et al. (2010) use receiver function data to supplement the area of the Amazon basin and image two distinct regions of thickened crust there. Some of this thickness is attributed to a possible mantle plume during the Paleozoic (Schmitz et al., 2002; Lloyd et al., 2010).

Like the other maps discussed here, our crustal thickness contour map (Fig. 3) shows clear definition of the continental margins of South America, particularly along the west coast. Whereas the western margin (the zone between the 10-km and 30-km contour lines) is narrow (<100 km), the eastern margin is locally much wider (up to ca. 1000 km or more). Even though the fit of the inferred continental margin to the Atlantic passive margin is not quite as exact (see above) as the fit to the Pacific convergent margin, both fits generally correspond well to the actual width and location of the continental shelves.

A simple average of the crustal thickness data used in the construction of Fig. 3 gives a value of 45.3 km for the average thickness of the South American continental crust, with a standard deviation of 13.1 km. However, there has been a disproportional amount of seismic research done in the Andes (e.g. James, 1971; Regnier et al., 1994; Beck et al., 1996; Dorbath, 1996; Myers et al., 1998; Yuan et al., 2000; Baumont et al., 2001; Bohm et al., 2002; Fromm et al., 2004; Alvarado et al., 2005; Heit et al., 2008; Wölbern et al., 2009) with the result that about half of the data comes from this restricted region. Thus, this thicker region is over-represented in the averaging process. Because instances of thinner crust in many other parts of South America are under-sampled, our above-calculated simple average value is more than 6 km greater than the global average of 39.2 km (Christensen and Mooney, 1995).

To compensate for the over-sampling of data in some regions of South America and the under-sampling in others, we have used the gridding function of commercial contour-mapping software Surfer 9 (Golden Software, 2009) on the original thickness data to create a set of uniformly spaced artificial thickness values. These values can then be appropriately weighted and averaged to find a truer result for the average continental crustal thickness under South America. We generated a grid of values that are uniformly spaced every 1° of latitude between 15° north latitude and 60° south latitude, and every 1° of longitude between 20° west longitude and 90° west longitude. Instead of letting the software construct

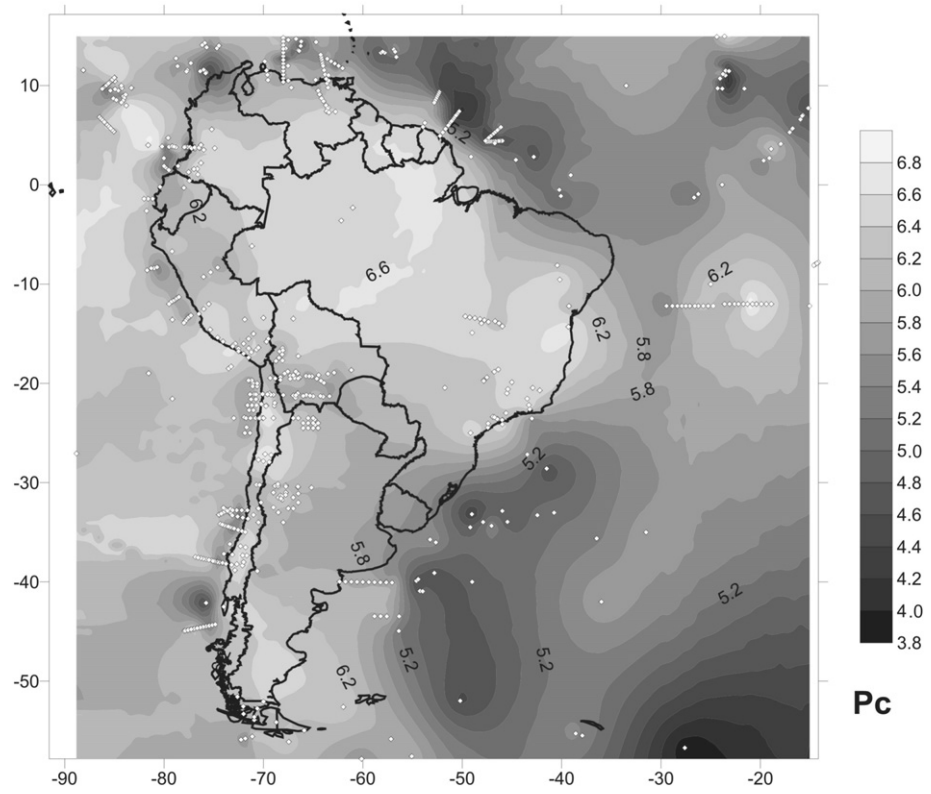

Fig. 4. Map of South America showing the average whole crustal P-wave velocity (P_c). White dots are datapoints/control locations. High average velocities seem prevalent in Colombia, southern Peru, the Amazonas Basin, northern-most Chile, and central Chile, while low average velocities appear to occur in central Peru, southern Bolivia, and southern Chile. However, the overall highest average velocities in the continent appear, as expected, under the shields, with the lowest values occurring in the major basins at the mouths of the Amazon River and Rio de la Plata. See Fig. 1 for location of place names.

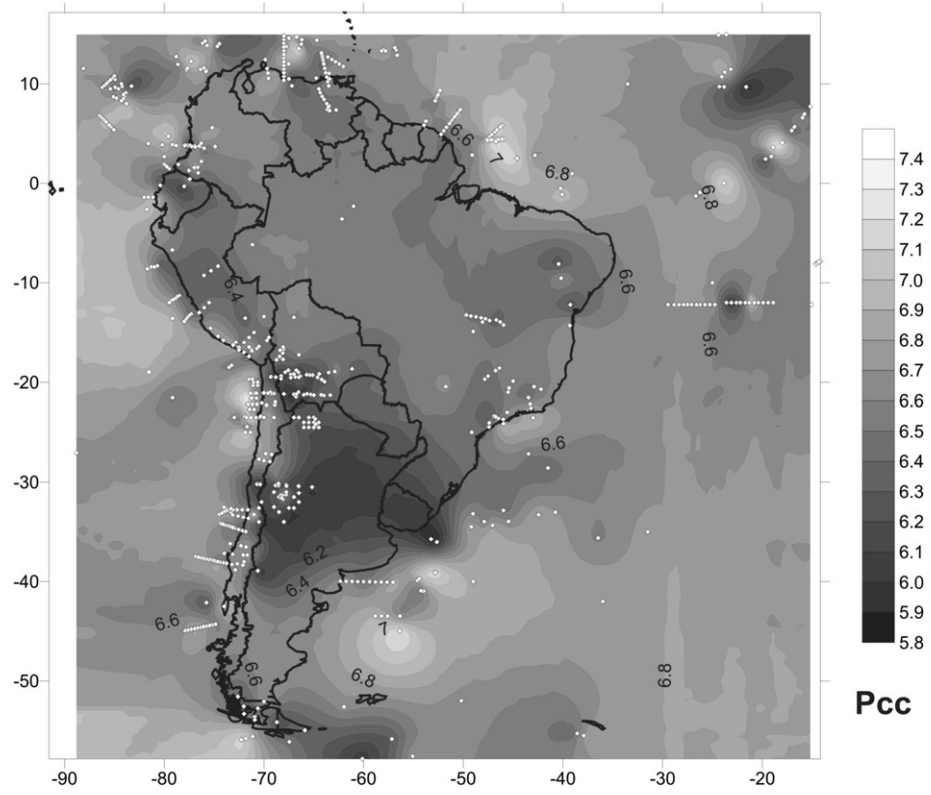

Fig. 5. Map of South America showing the average P-wave velocity (P_{cc}) of the crystalline crust. White dots are datapoints/control locations. The map clearly distinguishes granitic continental crust with lower velocities (generally <6.6 km/s) from gneissic oceanic layer 3 crust (generally >6.6 km/s). One very striking feature is the east-west band of continental crust between 25 degrees and 35 degrees south latitude, where the data seem to indicate a region with generally low average crystalline velocities (<6.2 km/s). Also, removing the sedimentary strata from the Atlantic side results in equivalent oceanic values.

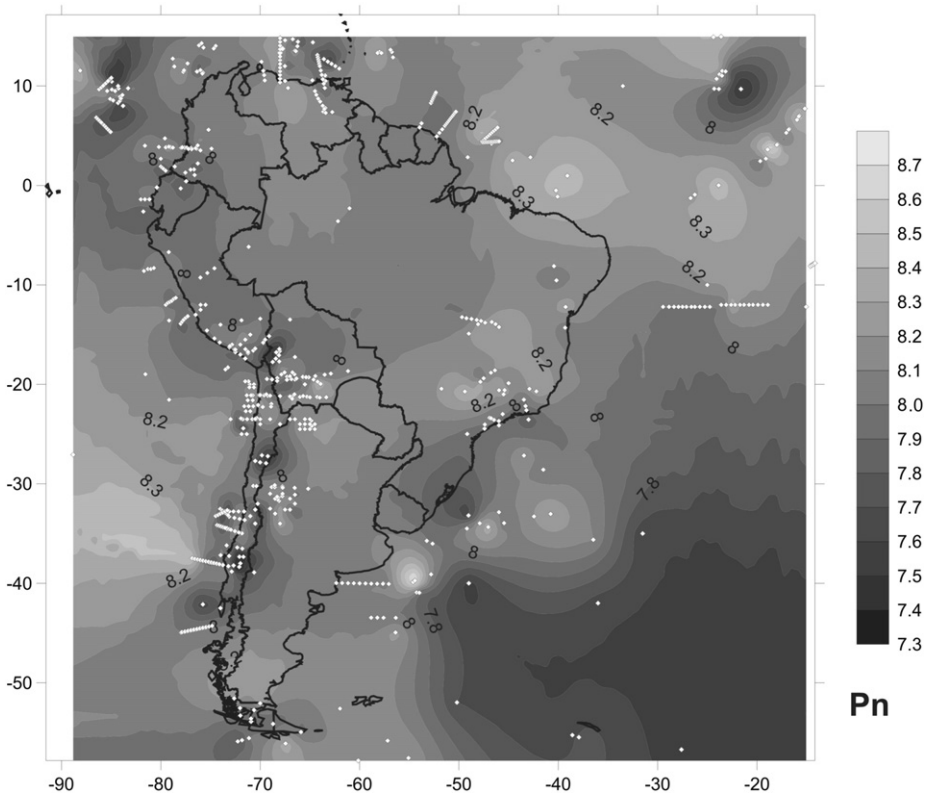

Fig. 6. Sub-Moho P-wave velocity (P_n) for South America. White dots are datapoints/control locations. Much of the continental interior is underlain by mantle with a P_n velocity of at least 8.0 km/s. The one notable exception to this pattern is within the Andes mountain chain. Most of the Andes are underlain by slightly slower mantle with P_n velocities <=8.0 km/s, but there is a disruption to this pattern between 20 and 30 degrees south latitude, possibly related to the Nazca plate "flat slab," although we do not observe a similar feature beneath the Peruvian "flat slab".

a contour map from the grid, we had it generate an ASCII file of the grid points. The resulting file contains three columns of data, the first being the latitude (θ_i) of each grid point, the second being the longitude, and the third being the crustal thickness value of the grid point (H_i), determined by natural-neighbor interpolation from the original scattered crustal thickness data. We then manually edited this ASCII file as described below.

To eliminate oceanic crustal values, we overlaid the elevation at each grid point. Points with an elevation below −0.5 km (more than 0.5 km below sea level) were assumed to be oceanic and, thus, eliminated. What remained was inspected by hand for anomalies. Virtually all of the anomalies discovered were assumed to be thickened oceanic crust and were, therefore, also eliminated.

Because we hoped to get a proper average for the crustal thickness using the H_i values, the grid points had to be uniformly spaced by linear distance rather than angular distance. Thus, we weighted each value by a factor of $\cos(\theta_i)$ to account for the narrowing of longitude with latitude. We then calculated the weighted average to find the average continental crustal thickness (H_c^{avg}) under South America using the formula:

$$H_c^{avg} = \sum_i H_i \cos(\theta_i) / \sum_i \cos(\theta_i) \quad (1)$$

The weighted standard deviation is then calculated using:

$$\text{S.D.} = \text{sqrt}\left(\frac{\sum_i^n \cos(\theta_i)\left(H_i - H_c^{avg}\right)^2}{\frac{N-1}{N}\sum_i^n \cos(\theta_i)} \right) \quad (2)$$

Using Eq. (1), we find that $H_c^{avg} = 38.17$ km, which is about 1 km less than the global average continental crustal thickness of 39.2 km determined by Christensen and Mooney (1995). We can calculate a "simple" weighted standard deviation for H_c^{avg} by multiplying the above standard deviation by H_c^{avg} and dividing by the simple mean (Eq. (2)). Thus, the weighted standard deviation (S.D.) is 8.7 km.

4.2. Average whole crustal P-wave velocity (P_c)

The average whole crustal P-wave velocity under South America and the surrounding ocean basins is presented in Fig. 4. This contour map confirms the existence of a contrast between the relatively low average crustal velocity (often less than 6.0 km/s) of the Atlantic seafloor and the relatively high velocity (often greater than 6.4 km/s) of the eastern Pacific seafloor found by Chulick and Mooney (2002). This contrast appears to be due to the greater thickness of sediment on the older, Atlantic seafloor (e.g. Blaich et al., 2011) formed at a slowly-opening mid-ocean ridge, as opposed to the younger, eastern Pacific seafloor formed at a faster-opening mid-ocean ridge (see cross sections shown in Fig. 12a–f). The combined data clearly delineates large, deep low-velocity sedimentary basins off the mouth of the Amazon, and on the South Atlantic, whereas it only shows narrow low-velocity regions in the South Pacific that correspond to trench fill.

Inside the continent, the map shows a pattern of varying average crustal velocities along the length of the Andes. These alternating "bands" of high and low seismic velocities in the mountains have been noted regionally by a number of investigators (e.g. Wigger et al., 1994; Schmitz, 1994; Yuan et al., 2000, 2002; Baumont et al., 2001, 2002; Beck and Zandt, 2002; ANCORP Working Group, 2003), but

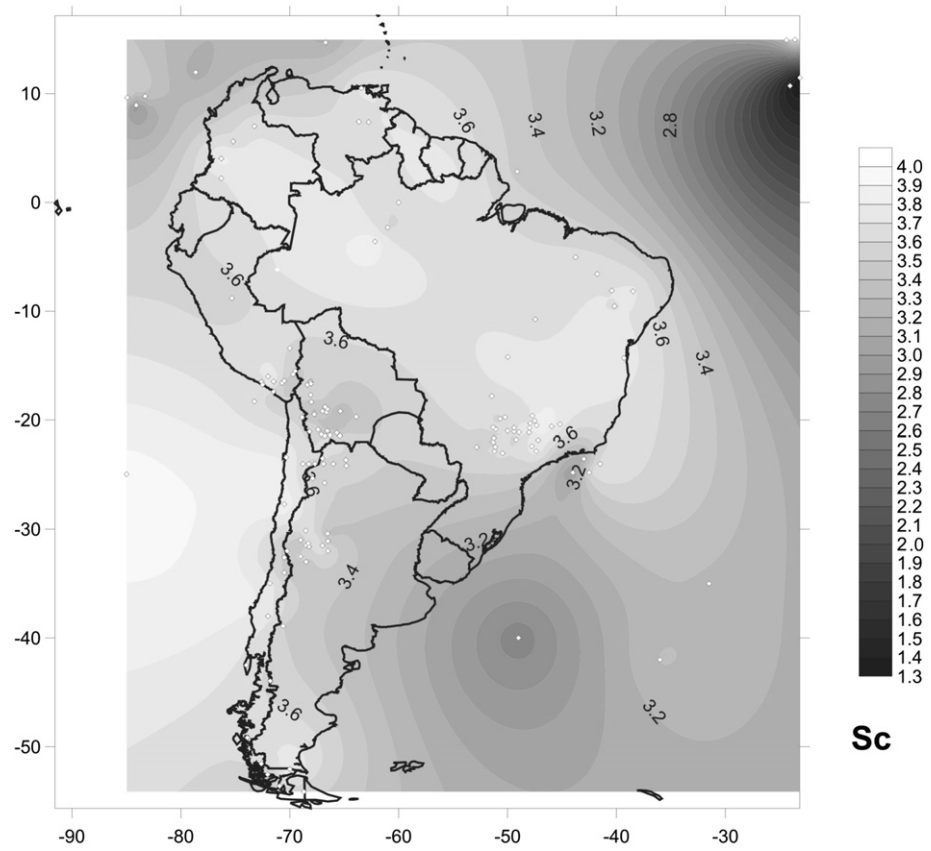

Fig. 7. Map showing the average crustal S-wave velocity (S_c) for South America. White dots are datapoints/control locations. The most striking feature is the strong contrast in average S-wave crustal velocity between the northern (>3.5 km/s) and southern (<3.5 km/s) halves of the continent. Also, the S-wave map hints at velocity variations along local segments of the Andes such as high S_c velocities (>3.5 km/s) in the Austral Andes, but lower S-wave velocities (3.0–3.5 km/s) in the central Chilean Andes and Pampean flat slab region.

our map assembles into one picture the overall pattern along the entire chain. High average velocities seem prevalent in Colombia, southern Peru, northern-most Chile, and central Chile. There seem to be lower velocity regions in Ecuador, central Peru (note that the three data points there are earthquake models), southern Bolivia (~20°S) and central Chile (30° to 35°S). In the northern Andes there may be a correlation between thick crust and high velocities. The low average velocities that occur in north and central Peru, and north-central Chile appear to correlate with the Peruvian and Chilean (Pampean) flat slab regions. However, due to the scarcity of data in north and central Peru (see above) there is not a clear correlation between low velocity and the Peruvian flat slab, and so no definite conclusions can be reached on this point. There is a much higher correlation between low P_c velocity and the Pampean flat slab due to the large amount of data available in that area. In fact, the data strongly suggests that the velocity distribution is actually "target-like" with a high velocity "bullseye" surrounded by lower velocities in the western portion of the Pampean flat slab region.

As expected, the overall highest average velocities in the continent appear under the shields. A band of high velocity (>6.6 km/s) crust can be seen through central Brazil, though this is likely a contouring artifact due to a lack of data in this region. Nonetheless, the velocities in this region are probably at least 6.4 km/s (the >6.6 km/s contour in far east Brazil is certainly real, but poorly-defined due to the scarcity of data along this stretch of coast).

Finally, we see a close correspondence between continental regions of high average crustal velocity and compressional orogens. We may also reproduce the previously known close correspondence between extended and/or rifted crust and regions of low average crustal velocity when we consider the NW Argentina Pre-cordillera, the mouth of the Amazon basin, and lower Rio de la Plata valley.

4.3. Crystalline crustal P-wave velocity (P_{cc})

Regions underlain with thick accumulations of low-velocity sediments strongly influence the contour map of whole-crustal P-wave velocity seen in Fig. 4. Thus, we have also calculated the average P-wave velocity in the crystalline crust (i.e., below surficial sediments and sedimentary rocks, here taken as $V_p < 5.8$ km/s). The map (Fig. 5) clearly distinguishes granitic continental crust, which has relatively lower velocities (generally <6.6 km/s, Christensen and Mooney, 1995), from gneissic oceanic layer 3 crust (generally >6.6 km/s). This confirms the findings of Chulick and Mooney (2002) in North America. The P_{cc} data also makes clear that the Andean Basement is generally lower in velocity than the shields as well (with exceptions in western Colombia and northern Chile – a clear indicator of velocity segmentation along the Andes).

One very striking feature of this map is the east-west band of continental crust between 25 degrees and 35 degrees south latitude. Here the data seems to indicate a region with generally low average crystalline velocities (<6.2 km/s). This region is underlain by a flat slab of the subducting Nazca plate, which corresponds to a gap in the Andean volcanic arc (e.g. Isacks et al., 1968; Cahill and Isacks, 1992; Ramos et al., 2002; Gilbert et al., 2006; Gans et al., 2011). This region could be analogous to the southwest United States, where a flat slab portion of the ancient Farallon plate may

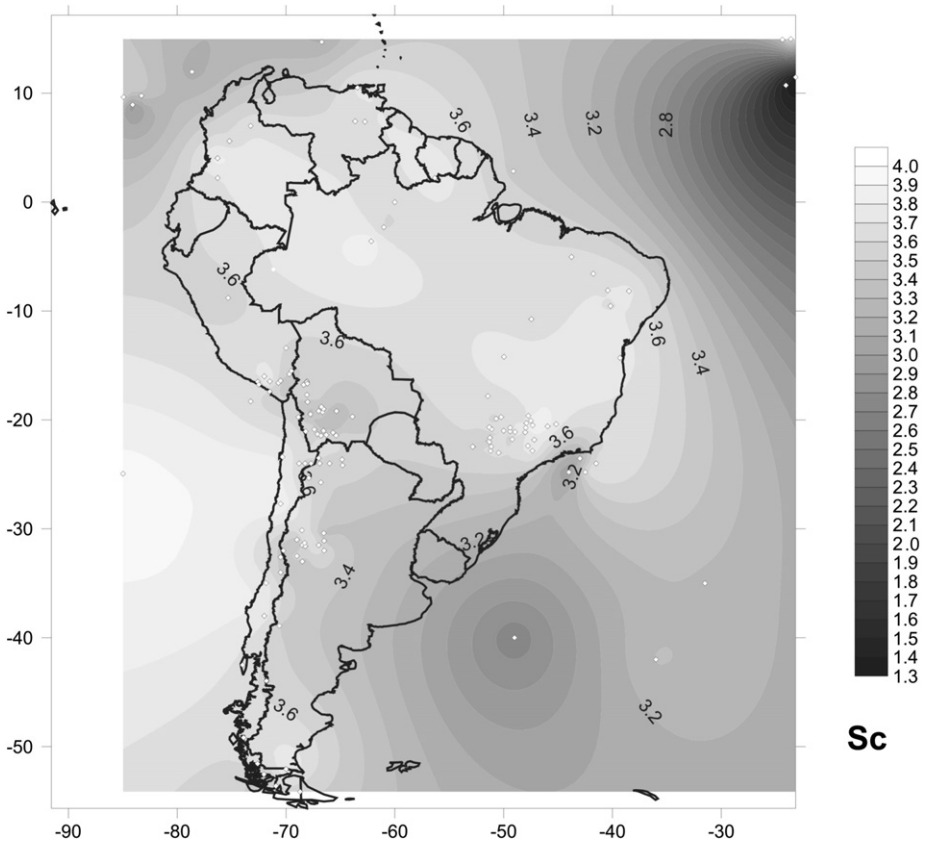

Fig. 8. Average S-wave velocity (S_{cc}) for the crystalline crust of South America. White dots are datapoints/control locations. The most striking feature unveiled here is the low velocity (<3.5 km/s) zone likely corresponding to the Pampean flat slab region under Northern Chile and Argentina also stands out. The results for S_{cc} under the Andes are again consistent with our previous observations about "velocity bands" or velocity variations along different segments of the range.

underlay the region (e.g. Helmstaedt et al., 2004; Gorbatov and Fukao, 2005). Just like in the southwest United States, there is a "Basin and Range" province located above this flat slab region of South America; the North American Basin and Range is similarly underlain by very low velocity (<6.2 km/s), high heat flow crystalline crust (Beck et al., 2005). Once again, because of a scarcity of data, no such conclusion can be reached about the more northerly Peruvian "flat slab." At best, there is just a hint of possible low P_{cc} velocities in this region.

Finally, note in general that P_{cc} velocities are lower in southern South America than in the northern shield regions. This is not due merely to especially low velocity, but also several other nearby regions with low P_{cc}, including northernmost Chile and the continental shelf of Uruguay.

Another feature that appears on this map in the eastern Pacific Ocean is the Nazca Ridge, which appears here as a region with anomalously low velocity (<6.6 km/s) layer 3 oceanic crust.

The global average P-wave velocity was found to be 6.45 km/s (Christensen and Mooney, 1995), and we find good agreement for the continent of South America (6.47 km/s). Since the average crystalline crustal velocity is related to the composition of the crust, the apparent global conformity of this parameter strongly supports the hypothesis that crustal formation has been a uniform process on a global scale for at least the past 3.0 billion years (Ga).

4.4. Sub-moho P-wave velocity (P_n)

The contour map of P_n, the seismic velocity of the uppermost lithospheric mantle, is presented in Fig. 6. It is important to observe that there is insufficient azimuthal coverage to make corrections for seismic anisotropy. This is undoubtedly one reason why this map shows many small-scale features. The continental-scale variation in P_n velocity is anyway more likely attributable to variation in lithospheric temperature (e.g., Artemieva and Mooney, 2001), than to anisotropy. Nonetheless, several features are discernable in this map.

Much of the continental interior is underlain by mantle with a P_n velocity of at least 8.0 km/s. The one notable exception to this pattern is the Andes Mountains. The Andes tend to be underlain by slightly slower upper mantle velocities ($P_n < 8.0$ km/s) than the rest of the continental interior. This anomaly is likely related to Andean subduction processes, as this phenomenon has been observed elsewhere at subduction zones (e.g., Iwasaki et al., 1994; Hyndman et al., 2005) and could be indicative of serpentinization of the mantle (Barklage et al., 2006). A minor disruption to this pattern under the Andes mountains occurs at about 30 degrees south latitude where velocities are >8.0 km/s, but this may be related to the Pampean flat slab discussed elsewhere in this paper. Thus, this pattern of behavior may reflect such features as low-velocity above-slab mantle channels and slab geometry.

P_n along the Chilean coast and western edge of the Andes is generally quite low, with exceptional higher velocity segments at about 22° S and 30° S. This may be a feature associated with differences in subduction along the Chilean Coast versus Central Peru. There is a hint that the Ecuadorian/Colombian Coast may be similar to Chile. We also note that data in southern Brazil suggests that P_n is also relatively low along the SE coast of Brazil.

Continental-scale variations in P_n velocity largely correlate with the thermal state of the lithosphere, with lower P_n velocities associated with higher lithospheric temperatures (e.g., Mooney and

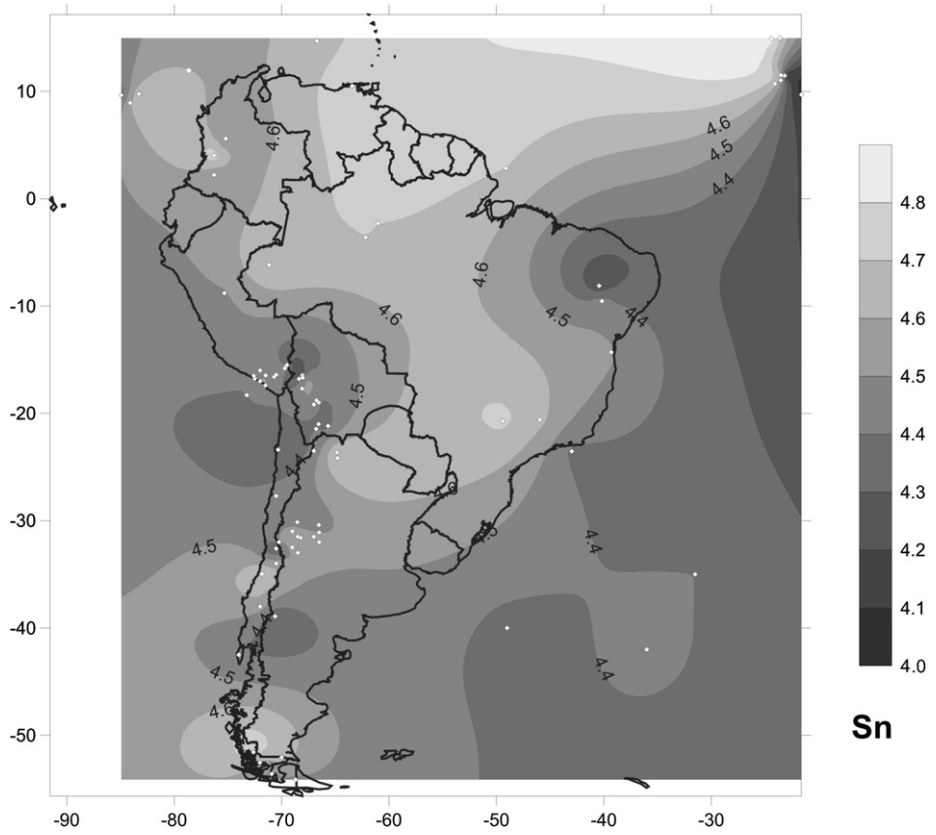

Fig. 9. Map showing the average Sub-Moho S-wave velocity (S_n) of South America. Only 90 datapoints (white dots) were available to construct this map so it should be considered as preliminary. Cursory examination of the S_n map indicates high velocities under the shields (old, cold craton), and low velocities under the Andes (warm, low-velocity above-slab mantle channels) as would be expected.

Braile, 1989), as under portions of the Andes or by the presence of water. For example, the higher P_n under the north central Chilean Andes could imply lower temperatures associated with the lack of volcanism attributed to the "flat slab". We observe that high P_n values (>8.0 km/s) are found in the Brazilian Shield and under much of the seafloor, while very low P_n values (<7.8 km/s) are found beneath the region of the Argentine Basin and possibly under the Chile Rise as it subducts.

4.5. Average crustal S-wave velocity (S_c)

There are substantially fewer available values of average whole-crustal S-wave velocity (S_c) than of P_c. Given the sparse quantity of data (142 values), contour maps of S_c should be interpreted with caution.

The location of data points and contours of S_c for South America are shown in Fig. 7. The most striking feature is the strong contrast in average S-wave crustal velocity between the northern (>3.5 km/s) and southern (<3.5 km/s) halves of the continent. A similar velocity dichotomy also appears in the average crustal P-wave map (Fig. 4), but is somewhat obscured by the greater local detail on that map due to the higher density of P-wave data available.

Furthermore, the S-wave map suggests possible velocity variations along local segments of the Andes, similar to those revealed in the P-wave maps. For example, high S_c (>3.5 km/s) appears probable in the Austral Andes. In contrast, lower S-wave velocities (<3.5 km/s) appear in the central Chilean Andes and the Pampean flat slab region under northern Chile and Argentina, and under southern Bolivia. These low S_c regions generally correlate with the low P_c regions, and so likely correspond to areas with high heat flow (discussed above) and/or extended crust (discussed below).

The lack of published S-wave crustal data for the seafloor limits the observations we can make. Several models exist for the Argentine Basin that strongly suggest S_c should be low in this region (~3 km/s or less), which is consistent with this being a sedimentary basin. The lack of such data models for the Brazil Basin causes the gridding software (and subsequent contours) to unrealistically calculate an anomalously high velocity for this region. The 3.6 km/s contour follows very well much of the edge of the continent along the Atlantic Coast (and seems to be associated with the western edge of the Brazilian Craton).

4.6. Crystalline crustal S-wave velocity (S_{cc})

The average crustal S-wave velocity in the crystalline crust (S_{cc}, see Fig. 8) was calculated in a manner analogous to that for the P_{cc} velocity. Here, we assume that a minimum value of 3.35 km/s ($V_p/V_s = 1.73$) defines the top of the crystalline crust.

There are several striking features revealed by this map. First, the western Amazon Basin region exhibits relatively high S_{cc} values (>3.8 km/s), whereas much of the shield regions display somewhat lower velocity (3.6–3.7 km/s) crust. A closer look at the Brazilian shield reveals localized variations in S_{cc}, with a general increase from ~3.6 km/s in the interior to ~4 km/s near the coast.

Perhaps the most remarkable feature shown here is the low velocity (<3.5 km/s) zone that corresponds to the flat slab region under Northern Chile and Argentina. Low S_{cc} values are consistent with the discussion above concerning low P_{cc}, in the Basin and

Range Province of the southwestern United States. The low velocity region appears quite extensive and is divided in half by a N–S higher velocity "ridge" which appears to coincide with the P-wave "bullseye" of the Pampean flat slab (see above). Additional data in southern Bolivia has also clearly unveiled an extended region of very low S_{cc}.

The results for S_{cc} under the Andes are again consistent with our previous observations about "velocity bands" or velocity variations along segments of the Andes for P-wave models. In general S_{cc} appears to be quite slow beneath the Andes. Higher S_{cc} (>3.75 km/s) occurs under the Northern and Austral Andes, while lower S_{cc} (<3.75 km/s) occurs from central Peru with slight evidence through central Chile (in the Altiplano and the two flat slab regions, see discussion above). An additional lateral velocity gradient from west (<3.7 km/s) to east (>3.8 km/s) across the southern Brazilian Shield can also be seen. In contrast, the relatively high S_{cc} under much of the Brazilian shield, S_{cc} is apparently still at least 0.1 km/s slower under the Guiana Shield. Finally, the few S-wave models available for oceanic crust (as in the Argentine Basin) clearly reveal oceanic layer 3 on this map as areas of extremely high S_{cc} (~3.9 km/s).

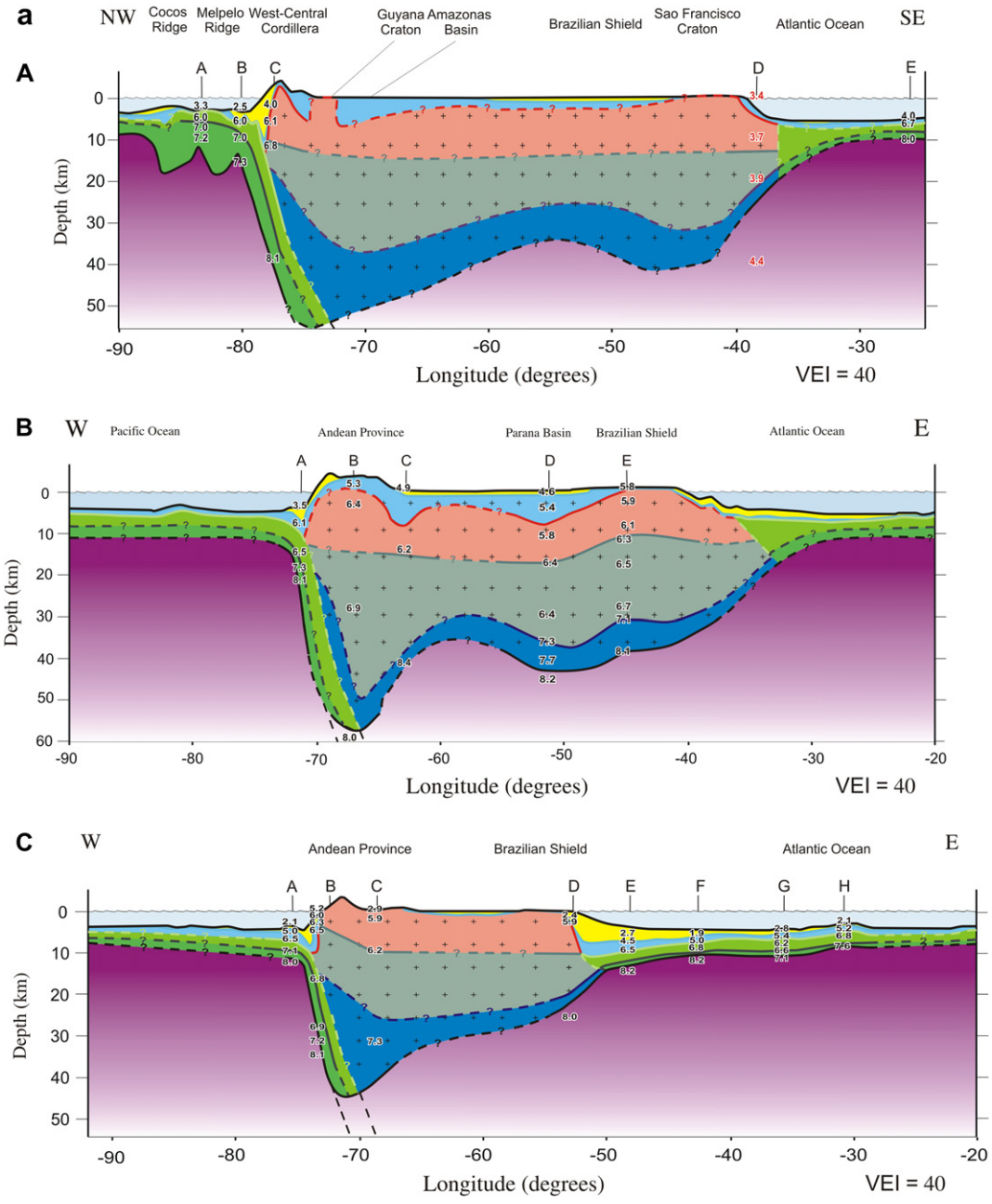

Fig. 10. Cross sections through the South American continent. Letters represent velocity profiles on or near the cross section line while the numbers show the velocities (black = from P-wave datapoints; red = from S-wave datapoints) in those locations. All datapoints lie within 300 km of the cross section line. (A) Across the Brazilian Shield (vertical exaggeration is ~110×). (B) At latitude 20 degrees south (vertical exaggeration is ~110×). (C) At latitude 33.5 degrees south (vertical exaggeration is ~130×). (D) At latitude 55 degrees south (vertical exaggeration is ~130×). (E) (Near the Atlantic coast, (vertical exaggeration is ~200×). For all maps the light blue and yellow areas show the sedimentary layers. The red area shows the upper crust, the green area shows the middle crustal layer, and the dark blue area shows the lower crust. All layers were interpolated between data points using the velocity constraints described in the text.

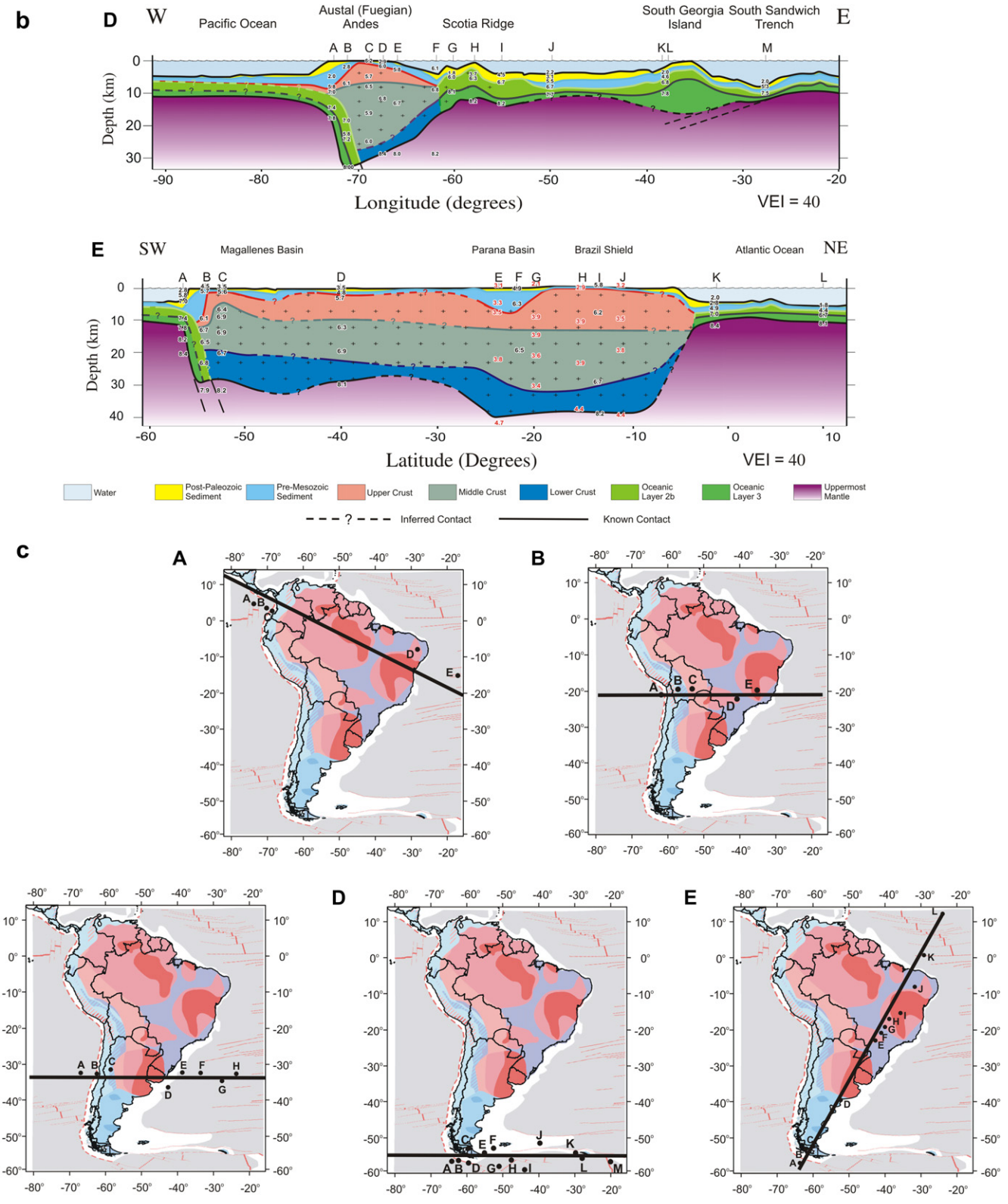

Fig. 10. (*continued*).

4.7. Sub-Moho S-wave velocity (S_n)

Only 79 data points are available to define the contour map of S_n velocity beneath South America (Fig. 9). Given the scarcity of data, this map should be considered as preliminary.

Cursory examination of the S_n map (Fig. 9) and P_n map (Fig. 6) indicates a gross similarity in distribution of high and low velocity values—high velocities under the shields (old, cold craton), and low velocities under the Andes (warm, low-velocity, above-slab mantle wedge). Still, there is some hint that there are higher velocity segments along the mountain chain – under perhaps Colombia (1 point), central Chile (1 point), and the southern tip of South America (definitely a change of regime here).

Nonetheless, there are several differences between the two contour maps, the most notable of which is that, while there is clear evidence for high P_n in the Pampean flat slab region under the Andes, there seems to be evidence for relatively lower S_n values. Close examination of both maps and of the database velocity depth models shows several data points in the region that have high P_n, but relatively low S_n.

When Fig. 9 is compared to the 100-km depth S-wave velocity map of SA99 (van der Lee et al., 2001, 2002), there are apparent gross similarities. At 100 km depth, SA99 shows fast mantle underlying the continental interior, surrounded by slow mantle underlying much of the continental margins. Our map of S_n shows a similar pattern, with higher S_n under the interior and lower S_n closer to the margins.

4.8. Crustal velocity structure cross-sections

Fig. 10 shows five cross sections through the South American continent synthesized from nearby individual velocity depth functions. The locations of the cross-sections are shown in the figure insets, and are located roughly through the Brazilian shield, at 20 degrees south latitude, at 33.5 degrees south latitude, at 55 degrees south latitude, and along the South American Atlantic coast. Vertical exaggeration varies by cross section. To construct the cross-sections, we developed contour maps in the following manner.

We selected a series of P-wave velocity horizons at 4.0, 5.8, 6.2, and 6.6 km/s, (which roughly correspond to post-Paleozoic sediments, the top of the crystalline continental crust or oceanic layer 2b crust, the top of the middle crust, and the top of high-velocity lower continental crust or layer 3 oceanic crust). We then applied these to the one-dimensional velocity-depth functions in the database to determine the depths at which these horizons occur. Then, along with elevation data (provided by ETOP02, National Geographic Data Center, 2001) and with the Moho depth, we used the software to construct a series of contour maps of depth to these various horizons (using a linear interpolation between points) with respect to sea level. By using the SLICE function of the software and overlaying the "slices" for each contour map, we were able to construct the desired cross-sections.

To help in the interpretation of the cross-sections, we have overlaid a selection of one-dimensional velocity depth functions from the database that fall within a certain geographical tolerance (300 km) of each cross section line (black—P-wave data; red—S-wave data). Many of the physical properties of the continent (such as details of the sedimentary layers, the Pampean flat slab, and the thick crustal root beneath the Andes Mountains) can be seen in the cross-sections.

The bulk of the data in the region of Pampean flat-slab subduction is derived from the CHARGE (e.g. Wagner et al., 2005; Alvarado et al., 2009) and CHARSME (e.g. Monfret et al., 2005; Deshayes et al., 2008) experiments. The model we

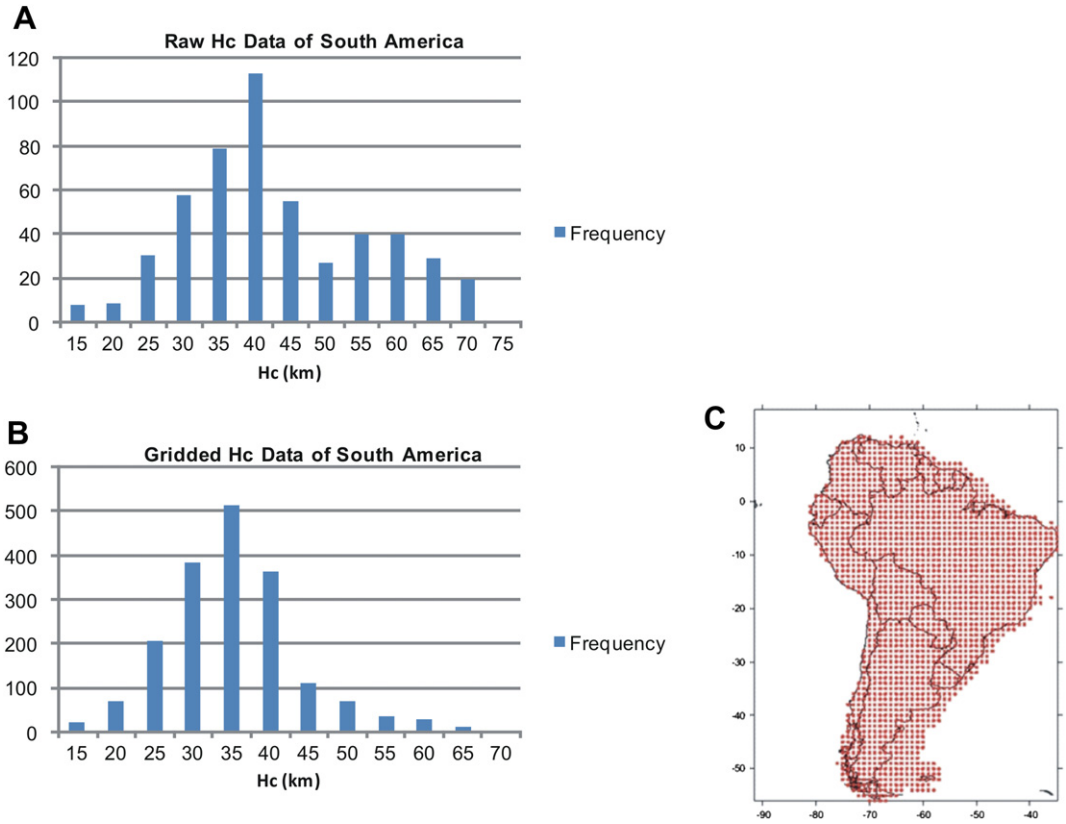

Fig. 11. Histogram of the raw (a) and gridded (b) crustal thickness data (H_c) of the crust in South America. The one degree gridding (shown in c) was used to average the thickness data over the entire continent. Otherwise, since most of our data points are in the thicker Andean regime, our average thickness for the continent would be skewed.

constructed from the contouring software reveals a bullseye pattern on the P_{cc} map (Fig. 5), consisting of concentric rings of decreasing velocity (down to <6.0 km/s) surrounding a central region (dome) of much higher velocity (>6.4 km/s) centered at approximately 32°S, 68°W. This is consistent with the results presented in Alvarado et al. (2009). The dome coincides with the Cuyana Terrane, a region Alvarado et al. (2009) identify as having thick 60 km crust (~50 km in our model), with a relatively high lower-crustal compressional wave velocity of 6.5 km/s (represented by the dome in our model). It also has a high V_p/V_s ratio of 1.83 (6.4/3.5 = 1.81 in our model), which sits 100 km above and approximately 200 km to the south of the heart of the flat-slab (see Figs. 1 and 2 of Alvarado et al., 2009).

Alvarado et al. (2009) contrast this region to the nearby Pampa Terrane, which lies to the northeast, centered near 30°S, 65°W. They have identified the Pampa Terrane as a region of average crustal thickness (~35 km; our model gives ~40 km), with a low compressional velocity of 6.0 km (~<6.0 km in our model) and a normal V_p/V_s ratio of 1.73 (6.0/3.5 = 1.71 in our model). They ascribe this difference to ecolgization of the lower crust of the Cuyana Terrane via hydration from fluids derived from the underlying Nazca slab.

4.9. Statistical analysis of the geophysical parameters

Statistical analyses of the seismic parameters appearing in the contour maps are presented in Tables 1 and 2. The ratio of some seismic parameters (P_c/S_c, P_{cc}/S_{cc}, and P_n/S_n), are also presented in Table 2. However, due to insufficient data coverage (many P-wave, 1-D velocity depth models do not have corresponding S-wave models and vice versa), these ratios are not presented in the form of contour maps. For comparison, we present the statistical analyses of Christensen and Mooney (1995) for all continents and of Chulick and Mooney (2002) for North America in Table 1. The work of Christensen and Mooney (1995) was based on a worldwide set of 560 continental seismic-refraction data points. Histograms of these seismic parameters are presented in Figs. 11 and 12.

For South America we found an average whole crustal P-wave velocity (P_{cc}) of 6.47 km/s (Table 1). Since the global average P_{cc} determined by Christensen and Mooney (1995) is only slightly lower (6.45 km/s), we believe that further analysis of P_{cc} data from other continents should arrive at a very similar result. Indeed, Chulick and Mooney (2002) also show close agreement for North America (6.44 km/s).

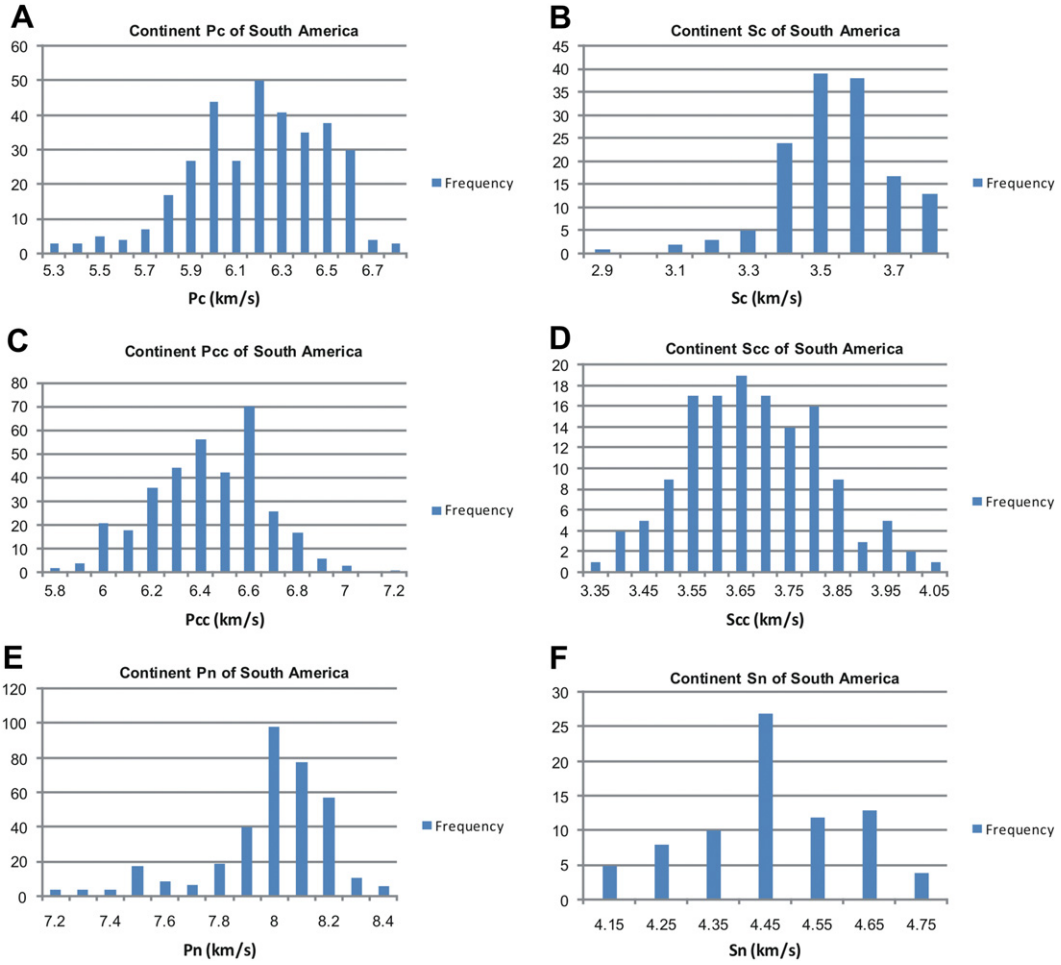

Fig. 12. a) Histogram of the P-wave velocity of the crust (P_c) in South America. Results show a slightly bimodal distribution at 6.00 and 6.20 km/s. b) Histogram of the S-wave velocity of the crust (S_c) in South America. Note the slight bimodality at 3.50 and about 3.62 km/s. c) Histogram of the P-wave velocity of the crystalline crust (P_{cc}) in South America, i.e. with sediments removed. Note the slightly bimodal distribution at 6.50 and about 6.80 km/s d) Histogram of the S-wave velocity of the crystalline crust (S_{cc}) in South America. Results show slight bimodality at 3.55 and near 3.70 km/s. e) Histogram of the P-wave velocity of the upper mantle (P_n) in South America. Note sharp peak between 8.00 and 8.10 km/s. f) Histogram of the S-wave velocity of the upper mantle (S_n) in South America.

The average value for P_n velocity under South America found by this study (8.00 km/s) is just slightly lower than the 8.07 km/s global average of Christensen and Mooney (1995), and very similar to the 8.02 km/s found for North America by Chulick and Mooney (2002). Given the large statistical populations used in these analyses, the various continental estimates of average P_n velocity appear to be well-determined values that are unlikely to change dramatically as additional measurements are compiled. It must be noted, however, that all of these statistical analyses assume a seismically isotropic mantle. An estimated 6% anisotropy will provide local azimuthally-dependent variations in P_n velocity of ±0.5 km/s (i.e., 7.5–8.5 km/s). Variations in mantle composition and especially in temperature are also important factors in determining P_n velocity (Artemieva and Mooney, 2001).

The histograms of the data used for the contour maps of Figs. 3–9 provide additional insights into the properties of the crust. The modal value of crustal thickness from the statistics and subsequent histogram for the original unweighted data is 43.83 km (Fig. 11a), a value that may be considered as thick crust on a global basis (Christensen and Mooney, 1995). As discussed above, this high modal value is skewed due to the numerous crustal profiles in Andean South America and the relative paucity of data from the middle of the continent. Fig. 11a shows that over half of all continental crustal thickness measurements exceed 40 km. However, a histogram constructed from 1832 grid points used to find the weighted average (Fig. 11b) produces a truer "bell-shaped curve," with a modal value of ~38 km, near the weighted average value of 38.17 km. This weighted average is the value for H_c given in Table 2.

The histogram for P_c (Fig. 12a) shows two modest peaks. This is also hinted at in the histogram for S_c (Fig. 12b) as well as that for P_{cc} and S_{cc} (Fig. 12c and d), demonstrating that the average velocity of the South American continental crust is bi-modal for both P- and S-waves. Our global database shows that similar plots of P_{cc} for all the other continents (with the exception of Antarctica, where data are extremely sparse) display the same bi-modality (Chulick and Mooney, 2002). We interpret this bi-modality as indicating the probable existence of two end-member types of continental crust. What distinguishes these two crustal types is the presence or absence of a high-velocity (6.9–7.3 km/s) lower crustal layer. Thin (20–35 km) crust commonly lacks a high-velocity lower crustal layer and has a low (~<6.5 km/s) average crustal velocity as per P_{cc}. Thick (35–50 km) crust, particularly that of stable continental interiors (i.e., platforms and shields), often has a high-velocity lower crustal layer and therefore, has a relatively high (~>6.5 km/s) average crustal velocity (Meissner, 1986; Mooney et al., 1998). Together, these two crustal types provide a global average of continental crustal velocity of 6.45 km/s.

P_n velocity peaks sharply around the average value of 7.998 km/s (Fig. 12e). More than 75% of all of the measurements of P_n velocity fall in the range 7.8–8.2 km/s, as anticipated from anisotropy considerations. The S_n velocity peaks around 4.50 km/s (Fig. 12f), near the statistical average of 4.504 km/s (Table 2).

5. Conclusions

We present new contour maps and a statistical analysis of the seismic structure of the crust and uppermost mantle of South America and the surrounding ocean basins. These results are based on a large number of new seismic measurements, including data from some previously unexplored regions. We have primarily used results from seismic-refraction surveys, with additional data acquired primarily from earthquake tomography studies, surface-wave analyses, and receiver functions (Table 3). From our analysis we conclude:

1) The weighted average of 889 measurements of continental crustal thickness (H_c) for South America is 38.17 km. This is ~1 km less than the global average of 39.2 km (Christensen and Mooney, 1995) and reflects the inclusion into our analysis of both numerous marine measurements made on the shallow and thin (20–25 km) continental shelf, as well as the thicker Andean crust.
2) Histograms of whole crustal average P- and S-wave velocities of the crystalline crust are generally bi-modal. A lower average crustal velocity (~<6.5 km/s) correlates with thin crust that lacks a high-velocity (6.9–7.3 km/s) lower crustal layer. A higher average crustal velocity (~>6.5 km/s) correlates with the moderately thick (~40 km) crust of the continental interior that includes a high-velocity basal crustal layer.
3) The average P-wave velocity of the eastern Pacific Ocean crust is higher than that of the western Atlantic Ocean crust due to a thinner sediment layer (layer 1) in the eastern Pacific Ocean. This supports a similar observation by Chulick and Mooney (2002) for the Atlantic and Pacific Ocean basins off North America.
4) The average P-wave velocity of the crystalline crust of South America is found to be 6.47 km/s, which is nearly equal to the global average of 6.45 km/s determined by Christensen and Mooney (1995). Since the average crustal velocity is related to the composition of the crust, the uniformity of this parameter strongly supports the hypothesis that crustal formation has been a uniform process on a global scale for at least the past 3.0 Ga.
5) The average P_n velocity under South America is 8.00 km/s, with more than 75% of all measurements falling in the range of 7.8–8.2 km/s.
6) The thickness of the crust under the Andes is relatively large, but highly variable. The Andean crust ranges from more than 60 km thick beneath northern Colombia and the Altiplano, a possible Tibetan Plateau analog, to a minimum of 30 km at Tierra del Fuego.
7) There is some evidence given the shallow Moho depths that the crust is extended in the regions between the Andes and the Guiana and Brazilian Shields that typically have a crustal thickness >40 km.
8) There are strong variations in seismic velocity along the length of the Andes, suggesting localized modifications in the tectonics.
9) The region of South America above the Pampean flat slab segment of the subducting Nazca plate appears to be a modern analog to the tectonic regime of the southwestern United States. Apart from the previously recognized Basin and Range Province in the Pre-Cordillera, this region is underlain by very low P- and S-wave crustal velocities, along with thinned crust. Data coverage is insufficient to draw similar conclusions about the Peruvian flat slab region although hints of low velocity are observed.
10) Regional variations in oceanic crustal and upper mantle seismic velocities appear to distinguish certain oceanic geographic features, including the Nazca Ridge, the Chile Ridge, and the Argentine Basin.

The complete South American database and the associated list of source references may be obtained on the Internet from the authors at: http://earthquake.usgs.gov/research/structure/crust/sam.php.

Acknowledgements

Support for this study by the National Earthquake Hazards Program of the USGS is gratefully acknowledged. Reviews by Mark

Goldman, Christian Guillemot, Pat McCrory, Jesse Kass, Leah Campbell, and two anonymous reviewers from the journal were extremely insightful and useful. Additional thanks are due to Neil Fenning and Alex Ferguson for help with data compilation and figure editing.

References

Agudelo, W., Ribodetti, A., Collot, J.Y., Operto, S., 2009. Joint inversion of multi-channel seismic reflection and wide-angle seismic data; improved imaging and refined velocity model of the crustal structure of the north Ecuador-south Colombia convergent margin. J. Geophys. Res. 114, B02306. http://dx.doi.org/10.1029/2008JB005690.

Alvarado, P., Beck, S., Zandt, G., Araujo, M., Triep, E., 2005. Crustal deformation in the south central Andes backarc terranes as viewed from regional broad-band seismic waveform modeling. Geophys. J. Int. 163, 580–598.

Alvarado, P., Beck, S., Zandt, G., 2007. Crustal structure of the south-central Andes Cordillera and backarc region from regional waveform modeling. Geophys. J. Int. 170, 858–875.

Alvarado, P., Pardo, M., Gilbert, H., Miranda, S., Anderson, M., Saez, M., Beck, S., 2009. Flat slab subduction and crustal models for the seismically active sierras pampeanas region of Argentina. Memoir – Geological Society of America 204, 261–278. http://dx.doi.org/10.1130/2009.1204(12).

An, M., Assumpção, M.S., 2004. Multi-objective inversion of surface waves and receiver functions by competent genetic algorithms applied to the crustal structure of the Parana Basin, SE Brazil. Geophys. Res. Lett. 31, 1–4.

An, M., Assumpção, M., 2005. Effect of lateral variation and model parameterization on surface wave dispersion inversion to estimate the average shallow structure in the Parana Basin. J. Seismol. 9, 449–462.

ANCORP Working Group, 2003. Seismic imaging of a convergent continental margin and plateau in the Central Andes (Andean Continental Research Project 1996). J. Geophys. Res. 108, 25. http://dx.doi.org/10.1029/2002JB001771.

Artemieva, I.M., Mooney, W.D., 2001. Thermal thickness and evolution of the Precambrian lithosphere: a global study. J. Geophys. Res. 106, 16,387–16,414.

Assumpção, M., James, D., Snoke, A., 2002. Crustal thinknesses in SE Brazilian Shield by receiver function analysis: Implications for isostatic compensation. J. Geophys. Res. 107 (B1), 2-1–2-14. http://dx.doi.org/10.1029/2001JB000422.

Assumpção, M., An, M., Bianchi, M., França, G.S.L., Rocha, M., Barbosa, J.R., Berrocal, J., 2004. Seismic studies of the Brasília fold belt at the western border of the São Francisco Craton, Central Brazil, using receiver function, surface-wave dispersion and teleseismic tomography. Tectonophysics 388, 173–185.

Balling, N., 1995. Heat flow and thermal structure of the lithosphere across the Baltic Shield and northern Tornquist Zone. Tectonophysics 244, 13–50.

Barklage, M.E., Conder, J., Wiens, D., Shore, P., Shiobara, H., Sugioka, H., Zhang, H., 2006. 3-D seismic tomography of the Mariana Mantle Wedge from the 2003–2004 passive component of the Mariana subduction factory imaging experiment. EOS Trans. Am. Geophys. Union. 87, no. 52, Suppl. 26.

Bassin, C., Laske, G., Masters, G., 2000. The current limits of resolution for surface wave tomography in South America. EOS Trans. Am. Geophys. Union 81, F897. http://igppweb.ucsd.edu/~gabi/crust2.html.

Baumont, D., Paul, A., Zandt, G., Beck, S.L., 2001. Inversion of Pn travel times for lateral variations of Moho geometry beneath the Central Andes and comparison with the receiver functions. Geophys. Res. Lett. 28, 1663–1666.

Baumont, D., Paul, A., Zandt, G., Beck, S.L., Pedersen, B., 2002. Lithospheric structure of the Central Andes based on surface wave dispersion. J. Geophys. Res. 107, 2371. http://dx.doi.org/10.1029/2001JB000345.

Beck, S., Zandt, G., Myers, S., Wallace, T., Silver, P., Drake, L., 1996. Crustal-thickness variations in the Central Andes. Geology 24, 407–410.

Beck, S.L., Zandt, G., 2002. The nature of orogenic crust in the Central Andes. J. Geophys. Res. 107, 2230. http://dx.doi.org/10.1029/2000JB000124.

Beck, S., Gilbert, H., Wagner, L., Alvarado, P., Zandt, G., 2005. The Sierras Pampeanas of Argentina: a modern analog for the Laramide Rocky Mountains in the western U.S. Earthscope meeting, New Mexico.

Berrocal, J., Marangoni, Y., De Sa, N.C., Fuck, R., Soares, J.E.P., Dantas, E., Perosi, F., Fernandes, C., 2004. Deep seismic refraction and gravity crustal model and tectonic deformation in Tocantins Province, Central Brazil. Tectonophysics 388, 187–199.

Bezada, M.J., Schmitz, M., Jacome, M.I., Rodriguez, J., Audemard, F., Izarra, C., Broadband Ocean-Land Investigations of Venezuela and the Antilles Arc Region (BOLIVAR) Active Seismic Working Group, (III), 2008. Crustal structure in the Falcon Basin area, northwestern Venezuela, from seismic and gravimetric evidence. J. Geodyn. 45, 191–200.

Blaich, O.A., Tsikalas, F., Faleide, J.I., 2008. Northeastern Brazilian margin; regional tectonic evolution based on integrated analysis of seismic reflection and potential field data and modelling; geodynamics of lithospheric extension. Tectonophysics 458, 51–67.

Blaich, O.A., Faleide, J.I., Tsikalas, F., Franke, D., Leon, E., 2009. Crustal-scale architecture and segmentation of the Argentine margin and its conjugate off South Africa. Geophys. J. Int. 178, 85–105.

Blaich, O.A., Faleide, J.I., Tsikalas, F., 2011. Crustal Breakup and Continent–Ocean Transition at South Atlantic Conjugate Margins. J. Geophys. Res. 116 (B01402). http://dx.doi.org/10.1029/2010JB007686

Blundell, D., Freeman, R., Mueller, S. (Eds.), 1992. A Continent Revealed—The European Geotranverse. Cambridge Univ. Press, p. 275.

Bohm, M., Luth, S., Echtler, H., Asch, G., Bataille, K., Bruhn, C., Rietbrock, A., Wigger, P., 2002. The Southern Andes between 36° and 40° S latitude: seismicity and average seismic velocities. Tectonophysics 356, 275–289.

Bostock, M.G., 1999. Seismic imaging of lithospheric discontinuities and continental evolution. Lithos 48, 1–16.

Cahill, T., Isacks, B.L., 1992. Seismicity and the shape of the subducted Nazca plate. J. Geophys. Res. 97, 17503–17529.

Christensen, N.I., Mooney, W.D., 1995. Seismic velocity structure and composition of the continental crust: a global view. J. Geophys. Res. 100 (B7), 9761–9788.

Christeson, G.L., Mann, P., Escalona, A., Aitken, T.J., 2008. Crustal structure of the Caribbean-northeastern South America arc-continent collision zone. J. Geophys. Res. 113, B08104. http://dx.doi.org/10.1029/2007JB005373.

Chulick, G.S., 1997. Comprehensive seismic survey database for developing three-dimensional models of the Earth's crust, Seismo. Res. Lett. 68 (5), 734–742.

Chulick, G.S., Mooney, W.D., 2002. Seismic structure of the crust and Uppermost mantle of North America and Adjacent Ocean basins: a synthesis. Bull. Seis. Soc. Am. 92 (6), 2478–2492.

Collins, C.D.N., 1988. Seismic velocities in the crust and upper mantle of Australia, Bureau of Mineral Resources, Geol. Geophys. Rept. 277, Aust. Gov't. Publ. Service, Canberra, Australia, 159 pp.

Cordani, U.G., Teixeira, W., D'Agrella-Filho, M.S., Trindade, R.I., 2009. The position of the Amazonia craton in supercontinents. Gondwana Res. 15, 396–407.

Cordani, U.G., Teixeira, W., Tassinari, C.C.G., Coutinho, J.M.V., Ruiz, A.S., 2010. The Rio Apa Craton in Mato Grosso du Sol (Brazil) and Northern Paraguay: Geochronological Evolution, correlations and tectonic implications for Rodinia and Gondwana. Am. J. Sci. 310, 981–1023. http://dx.doi.org/10.2475/09.2010.09.

Deshayes, P., Monfret, T., Pardo, M., Vera, E., 2008. Three-dimensional P- and S-wave seismic attenuation models in central Chile – western Argentina (30° – 34° S) from local recorded earthquakes. In: 7th International Symposium on Andean Geodynamics (ISAG, 2008 Nice, France) Extended Abstracts, pp. 184–187.

Dorbath, C., 1996. Velocity structure of the Andes of central Peru from locally recorded earthquakes. Geophys. Res. Lett. 23, 205–208.

Eaton, D., Mereu, R., Jones, A., Hyndman, R., 2005. The Moho beneath the Canadian Shield. Geophys. Res. Abst. 7, 05568.

Feng, M., Assumpção, M., van der Lee, S., 2004. Group-velocity tomography and lithospheric S-velocity structure of the South American continent. Phys. Earth Plan. Int. 147, 315–331.

Feng, M., van der Lee, S., Assumpção, M., 2007. Upper mantle structure of South America from joint inversion of waveforms and fundamental mode group velocities of Rayleigh waves. J. Geophys. Res. 112, B04312. http://dx.doi.org/10.1029/2006JB004449.

Flueh, E.R., Vidal, N., Ranero, C.R., Hojka, A., Von Huene, R., Bialas, J., Hinz, K., Cordoba, D., Danobeitia, J.J., Zelt, C., 1998. Seismic investigation of the continental margin off- and onshore Valparaiso, Chile. Tectonophysics 288, 251–263.

Fromm, R., Zandt, G., Beck, S.L., 2004. Crustal thickness beneath the Andes and Sierras Pampeanas at 30°S inferred from Pn apparent phase Velocities. Geophys. Res. Lett. 31, L06625. http://dx.doi.org/10.1029/2003GL019231.

Fuck, R., Bley Briton Eves, B., Schobbenhaus, C., 2008. Rodinia descendents in South America. Precambrian Res. 160, 108–126.

Gans, C.R., Beck, S.L., Zandt, G., Gilbert, H., Alvarado, P., Anderson, M., Linkimer, L., 2011. Continental and Oceanic Crustal Structure of the Pampean flat slab region, western Argentina, using receiver function analysis: new high-resolution results. Geophys. J. Int. 186, 45–58. http://dx.doi.org/10.1111/j.1365-246X.2011.05023.x.

Gilbert, H., Beck, S., Zandt, G., 2006. Lithospheric and upper mantle structure of central Chile and Argentina. Geophys. J. Int. 165, 383–398. http://dx.doi.org/10.1111/j.1365-246X.2006.02867.

Golden Software, 2009. Surfer 9. http://www.goldensoftware.com/products/surfer/.

Gorbatov, A., Fukao, Y., 2005. Tomographic search for missing link between the ancient Farallon subduction and the present Cocos subduction. Geophys. J. Int. 160, 849–854.

Greenroyd, C.J., Peirce, C., Rodger, M., Watts, A.B., Hobbs, R.W., 2007. Crustal structure of the French Guiana margin, West Equatorial Atlantic. Geophys. J. Int. 169, 964–987.

Heit, B., Yuan, X., Bianchi, M., Sodoudi, F., Kind, R., 2008. Crustal thickness estimation beneath the southern Central Andes at 30 S and 36 S from S wave Receiver Function Analysis. Geophys. J. Int. 174, 249–254.

Helmstaedt, H., Usui, T., Nakamura, E., Maruyama, S., 2004. Syn-Laramide UHP metamorphism under the Colorado Plateau; xenolith evidence for Proterozoic accretionary tectonics or flat subduction of the Farallon Plate? Abst. Progr. Geol. Soc. Am. 36, 210.

Hyndman, R.D., Currie, C.A., Mazotti, S., 2005. Subduction zone backarcs, mobile belts, and orogenic heat. GSA Today 15, 4–10.

Isacks, B., Oliver, J., Sykes, L., 1968. Seismology and the new Global Tectonics. J. Geophys. Res. 73, 5855–5899.

Iwasaki, T., Yoshii, T., Moriya, T., Kobayashi, A., Nishiwaki, M., Tsutsui, T., Iidaka, T., Ikami, A., Matsuda, T., 1994. Precise *P* and *S* wave velocity structures in the Kitakami massif, northern Honshu, Japan, from a seismic refraction experiment. J. Geophys. Res. 99, 22187–22204.

James, D.E., 1971. Plate tectonic model for the evolution of the Central Andes. Geol. Soc. Am. Bull. 82, 3325–3346.

James, D.E., Snoke, J.A., 1994. Structure and tectonics in the region of flat subduction beneath central Peru; crust and uppermost mantle. J. Geophys. Res. 99, 6899–6912.

Julia, J., Assumpção, M., Rocha, M.P., 2008. Deep crustal structure of the Parana Basin from receiver functions and Rayleigh-wave dispersion; evidence for a fragmented cratonic root. J. Geophys. Res. 113, B08318. http://dx.doi.org/10.1029/2007JB005374.

Lange, D., Rietbrock, A., Haberland, C., Bataille, K., Dahm, T., Tilmann, F., Flueh, E.R., 2007. Seismicity and geometry of the south Chilean subduction zone (41.5°S–43.5°S): Implications for controlling parameters. Geophys. Res. Lett. 34, 1–5.

Lawrence, J.F., Wiens, D.A., 2004. Combined receiver-function and surface wave phase-velocity inversion using a Niching Genetic Algorithm: application to Patagonia. Bull. Seis. Soc. Am. 94, 977–987.

Lloyd, S., van der Lee, S., França, G.S., Assumpção, M., Feng, M., 2010. Moho map of South America from Receiver Functions and Surface Waves. J. Geophys. Res. 115, B11315. http://dx.doi.org/10.1029/2009JB006829.

Meissner, R., 1986. The Continental Crust: A Geophysical Approach. Academic Press, London, 426 pp.

Monfret, T., Pardo, M., Salazar, P., Vera, E., Eisenberg, A., Yañez, G., 2005. Three dimensional P and S wave velocity models in central Chile and western Argentina (31°–34°S) from local data: no tear between the flat and steep segments of the Nazca plate. In: 6th International Symposium on Andean Geodynamics (ISAG 2005, Barcelona), Extended Abstracts, pp. 516–519.

Mooney, W.D., Meyer, R.P., Laurence, J.P., Meyer, H., Ramirez, J.E., 1979. Seismic refraction studies of the western cordillera Colombia. Bull. Seis. Soc. Am. 69, 1745–1761.

Mooney, W.D., 1989. Seismic methods for determining earthquake source parameters and lithospheric structure. In: Pakiser, L.C., Mooney, W.D. (Eds.), Geophysical Framework of the Continental United States. Geol. Soc. Am. Memoir, vol. 172, pp. 11–34.

Mooney, W.D., Braile, L.W., 1989. The seismic structure of the continental crust and upper mantle of North America. In: Bally, A.W., Palmer, A.R. (Eds.), The Geology of North America—An Overview. Geological Society of America, Boulder, CO, pp. 39–52.

Mooney, W.D., Laske, G., Masters, T.G., 1998. CRUST 5.1: a global crustal model at 5° x 5°. J. Geophys. Res. 103, 727–747.

Myers, S.C., Beck, S., Zandt, G., Wallace, T., 1998. Lithospheric-scale structure across the Bolivian Andes from tomographic images of velocity and attenuation for P and S waves. J. Geophys. Res. 103, 21233–21252.

Nascimento, A.F., Pearce, R.G., Takeya, M.K., 2002. Local shear wave observations in Joao Camera, Northeast Brazil. J. Geophys. Res. 107, 9. http://dx.doi.org/10.1029/2001JB000560.

Nataf, H.-C., Richard, Y., 1996. 3SMAC: an a priori tomographic model of the upper mantle based on geophysical modeling. Phys. Earth Planet. Int. 95, 101–122.

National Geographic Data Center, 2001. ETOP02. http://ols.nndc.noaa.gov/plolstore/plsql/olstore.prodspecific?prodnum=G02092-DVD-A0001 (accessed 05.02.12).

Ocola, L.C., Aldrich, L.T., Gettrust, J.F., Meyer, R.P., Raminez, J., 1975. Project Narino I: crustal structure under southern Colombian- Northern Ecuador Andes from seismic refraction data. Bull. Seis. Soc. Am. 65, 1681–1695.

Pakiser, L.C., Mooney, W.D., 1989. Introduction. In: Pakiser, L.C., Mooney, W.D. (Eds.), Geophysical Framework of the Continental United States. Memoir – Geological Society of America, vol. 172, pp. 1–9.

Patzwahl, R., Mechie, J., Schulze, A., Giese, P., 1999. Two-dimensional velocity models of the Nazca plate subduction zone between 19.5 S and 25 S from wide-angle seismic measurements during the CINCA95 project. J. Geophys. Res. 104, 7293–7317.

Pavlenkova, N.I., 1996. Crust and upper mantle structure in northern Eurasia from seismic data. Adv. Geophys. 37, 1–133.

Pavlenkova, N.I., Pilipenko, V.N., Verpakhovskaja, A.O., Pavlenkova, G.A., Filonenko, V.P., 2009. Crustal structure in Chile and Okhotsk Sea regions; deep seismic profiling of the continents and their margins. Tectonophysics 472, 28–38.

Prodehl, C., 1984. Structure of the earth's crust and upper mantle. In: Fuchs, K., Soffel, H., Hellwege, K.-H. (Eds.), Landolt Bornstein New Series – Physical Properties of the Interior of the Earth, the Moon and the Planets. Numerical data and functional relationships in science and technology. Group V, vol. 2a. Springer, Berlin-Heidelberg, pp. 97–206.

Ramos, V., Cristallini, E., Perez, D.J., 2002. The Pampean flat-slab of the Central Andes. J. South Am. Earth Sci. 15, 59–78.

Regnier, M., Chiu, J.M., Smalley, R., Isacks, B.L., Araujo, M., 1994. Crustal thickness variation in the Andean Foreland, Argentina, from Converted Waves. Bull. Seis. Soc. Am. 84, 1097–1111.

Rodger, M., Watts, A.B., Greenroyd, C.J., Peirce, C., Hobbs, R.W., 2006. Evidence for unusually thin oceanic crust and strong mantle beneath the Amazon fan. Geology 34, 1081–1084.

Scherwath, M., Flueh, E., Grevemeyer, I., Tilmann, F., Contreras-Reyes, E., Weinrebe, W., 2006. Investigating subduction zone processes in Chile. EOS 87, 265–269.

Schmitz, M., 1994. A balanced model of the southern Central Andes. Tectonics 13, 484–492.

Schmitz, M., Lessel, K., Giese, P., Wigger, P., Araneda, M., Bribach, J., Graeber, F., Grunewald, S., Haberland, C., Lueth, S., Roewer, P., Ryberg, T., Schulze, A., 1999. The crustal structure beneath the Central Andean forearc and magmatic arc as derived from seismic studies; the PISCO 94 experiment in northern Chile (21 degrees–23 degrees S). J. South Am. Earth Sci. 12, 237–260.

Schmitz, M., Chalbaud, D., Castillo, J., Izarra, C., 2002. The crustal structure of the Guayana Shield, Venezuela, from seismic refraction and gravity data. Tectonophysics 345, 103–118.

Schmitz, M., Martins, A., Izarra, C., Jácome, M.I., Sánchez, J., Rocabado, V., 2005. The major features of the crustal structure in north-eastern Venezuela from deep wide-angle seismic observations and gravity modeling. Tectonophysics 399, 109–124.

Schnabel, M., 2007. A deep seismic model for the Argentine continental margin. BGR. http://www.bgr.bund.de/cln_145/nn_336750/EN/Themen/MeerPolar/Meeresforschung/Projekte__und__Beitraege/Sued__Atlantik/seismic__model__argentina__en.html (accessed 12.22.09).

Soares, J.E., Berrocal, J., Fuck, R.A., Mooney, W.D., Ventura, D.B.R., 2006. Seismic characteristics of central Brazil crust and upper mantle: a deep seismic refraction study. J. Geophys. Res. 111, B12302,. http://dx.doi.org/10.1029/2005JB003769.

Tavera, H., Fernandez, E., Bernal, I., Antayhua, Y., Agueero, C., Rodriguez, H.S.S., Vilcapoma, L., Zamudio, Y., Portugal, D., Inza, A., Carpio, J., Callo, F., Valdivia, I., 2006. The southern region of Peru earthquake of June 23rd, 2001. J. Seismol. 10, 171–195.

van der Lee, S., James, D., Silver, P., 2001. Upper mantle S velocity structure of central and western South America. J. Geophys. Res. 106 (B12), 30821–30834.

van der Lee, S., James, D., Silver, P., 2002. Correction to "Upper mantle S velocity structure of central and western South America". J. Geophys. Res. 107 (B5). http://dx.doi.org/10.1029/2001JB001891

Wagner, L.S., Beck, S., Zandt, G., 2005. Upper mantle structure in the south central Chilean subduction zone (30° to 36°S). J. Geophys. Res. 110, B01308. http://dx.doi.org/10.1029/2004JB003238, pp. 1–20.

Wigger, P.J., Schmitz, M., Araneda, M., Asch, G., Baldzuhn, S., Giese, P., Heinsohn, W.-D., Martinez, E., Ricaldi, E., Roewer, P., Viramonte, J., 1994. Variation in the crustal structure of the southern central Andes deduced from seismic refraction investigations. In: Reutter, K.-J., Scheuber, E., Wigger, P.J. (Eds.), Tectonics of the Southern Central Andes (Structure and Evolution of an Active Continental Margin). Springer Verlag, p. 333.

Wölbern, I., Heit, B., Yuan, X., Asch, G., Kind, R., Viramonte, J., Tawackoli, S., Wilke, H., 2009. Receiver Function Images from the Moho and the slab beneath the Altiplano and Puna plateaus in the Central Andes. Geophys. J. Int. 177, 296–308.

Yoon, M., Buske, S., Shapiro, S.A., Wigger, P., 2009. Reflection image spectroscopy across the Andean subduction zone. Tectonophysics 472, 51–61.

Yuan, X.-C., 1996. Atlas of Geophysics in China. Geological Publishing House, Beijing, China, 217 pp.

Yuan, X., Sobolev, S.V., Kind, R., Oncken, O., Bock, G., Asch, G., Schurr, B., Graeber, F., Rudloff, A., Hanka, W., Wylegalla, K., Tibi, R., Haberland, C., Rietbrock, A., Giese, P., Wigger, P., Rower, P., Zandt, G., Beck, S., Wallace, T., Pardo, M., Comte, D., 2000. Subduction and collision processes in the Central Andes constrained by converted seismic phases. Nature 408, 958–961.

Yuan, X., Sobolev, S.V., Kind, R., 2002. Moho topography in the Central Andes and its geodynamic implications. Earth Planet. Sci. Lett. 199, 389–402.